Global Change Biology

Global Change Biology (2014) **20**, 3439–3456, doi: 10.1111/gcb.12640

Latent heat exchange in the boreal and arctic biomes

VILLE KASURINEN[1,2], KNUT ALFREDSEN[2], PASI KOLARI[1], IVAN MAMMARELLA[3], PAVEL ALEKSEYCHIK[3], JANNE RINNE[3], TIMO VESALA[3], PIERRE BERNIER[4], JULIA BOIKE[5], MORITZ LANGER[5], LUCA BELELLI MARCHESINI[6], KO VAN HUISSTEDEN[6], HAN DOLMAN[6], TORSTEN SACHS[7], TAKESHI OHTA[8], ANDREJ VARLAGIN[9], ADRIAN ROCHA[10], ALTAF ARAIN[11], WALTER OECHEL[12], MAGNUS LUND[13], ACHIM GRELLE[14], ANDERS LINDROTH[15], ANDY BLACK[16], MIKA AURELA[17], TUOMAS LAURILA[17], ANNALEA LOHILA[17] and FRANK BERNINGER[1]

[1]Department of Forest Sciences, University of Helsinki, POBox 27, Helsinki 00014, Finland, [2]Department of Hydraulic and Environmental Engineering, Norwegian University of Science and Technology, Trondheim, Norway, [3]Department of Physics, University of Helsinki, POBox 48, Helsinki 00014, Finland , [4]Natural Resources Canada, Canadian Forest Service, Stn. Ste-Foy, P.O. Box 10380 Quebec, QC G1V 4C7, Canada , [5]Alfred Wegener Institute, Helmholtz Centre for Polar and Marine Research, Research Unit Potsdam, Telegrafenberg, A 4314473 Potsdam, Germany, [6]Earth and Climate Cluster, Department of Earth Sciences, VU University Amsterdam, De Boelelaan 1085, Amsterdam 1081 HV, The Netherlands, [7]GFZ German Research Centre for Geosciences, Telegrafenberg, Potsdam 14473, Germany, [8]Graduate School of Bioagricultural Sciences, Nogoya University, Furo-cho, Chikusa Ward, Nagoya, Aichi 464-8601, Japan, [9]A.N. Severtsov Institute of Ecology and Evolution, Russian Academy of Sciences, Leninsky pr.33, Moscow 119071, Russia, [10]Department of Biological Sciences and the Environmental Change Initiative, University of Notre Dame, Notre Dame, IN 46556, USA, [11]McMaster Centre for Climate Change and School of Geography and Earth Sciences, McMaster University, Hamilton, Ontario, Canada, [12]Global Change Research Group, San Diego State University, 5500 Campanile Drive, San Diego, CA 92182, USA, [13]Arctic Research Centre, Department of Bioscience, Aarhus University, Frederiksborgvej 399, Roskilde DK-4000, Denmark, [14]Department of Ecology, Swedish University of Agricultural Sciences, Uppsala, Sweden, [15]Department of Earth and Ecosystem Sciences, Lund University, Lund, Sweden, [16]Faculty of Land and Food Systems, University of British Columbia, Vancouver, Canada, [17]Finnish Meteorological Institute, Atmospheric Composition Research, POBox 503, Helsinki Fi-00101, Finland

Abstract

In this study latent heat flux (λE) measurements made at 65 boreal and arctic eddy-covariance (EC) sites were analyses by using the Penman–Monteith equation. Sites were stratified into nine different ecosystem types: harvested and burnt forest areas, pine forests, spruce or fir forests, Douglas-fir forests, broadleaf deciduous forests, larch forests, wetlands, tundra and natural grasslands. The Penman–Monteith equation was calibrated with variable surface resistances against half-hourly eddy-covariance data and clear differences between ecosystem types were observed. Based on the modeled behavior of surface and aerodynamic resistances, surface resistance tightly control λE in most mature forests, while it had less importance in ecosystems having shorter vegetation like young or recently harvested forests, grasslands, wetlands and tundra. The parameters of the Penman–Monteith equation were clearly different for winter and summer conditions, indicating that phenological effects on surface resistance are important. We also compared the simulated λE of different ecosystem types under meteorological conditions at one site. Values of λE varied between 15% and 38% of the net radiation in the simulations with mean ecosystem parameters. In general, the simulations suggest that λE is higher from forested ecosystems than from grasslands, wetlands or tundra-type ecosystems. Forests showed usually a tighter stomatal control of λE as indicated by a pronounced sensitivity of surface resistance to atmospheric vapor pressure deficit. Nevertheless, the surface resistance of forests was lower than for open vegetation types including wetlands. Tundra and wetlands had higher surface resistances, which were less sensitive to vapor pressure deficits. The results indicate that the variation in surface resistance within and between different vegetation types might play a significant role in energy exchange between terrestrial ecosystems and atmosphere. These results suggest the need to take into account vegetation type and phenology in energy exchange modeling.

Keywords: eddy-covariance, evapotranspiration, latent heat, phenology, stomatal resistance

Received 31 January 2014 and accepted 13 March 2014

Correspondence: Ville Kasurinen, tel. +358-41-5343753, fax +358-9-191-58100, e-mail: ville.kasurinen@helsinki.fi

Introduction

Boreal and arctic biomes account for 22% of the land surface of the globe (Chapin *et al.*, 2000). Boreal landscapes are often considered to be dominated by evergreen needle leaf conifers, but broadleaf forests, larch forests, open areas also occupy large areas of the boreal and arctic biomes and wetlands occupy large areas of boreal and arctic domain. These boreal and arctic ecosystems play an important role in earth-atmosphere dynamics because of their large extent and their sensitivity to a warming climate (Chapin *et al.*, 2000; Bonan, 2008a).

Transpiration dominates the terrestrial ecosystem water fluxes and is poorly constrained in global modeling (Jasechko *et al.*, 2013). Nevertheless, global climate predictions are sensitive to changes in evapotranspiration (e.g., Sellers *et al.*, 1997, 2009). Over the last two decades, an extensive eddy-covariance (EC) flux tower network (FLUXNET) has been built, which is providing new insights on the energy exchange between the atmosphere and arctic and boreal ecosystems (Aubinet *et al.*, 2000; Baldocchi *et al.*, 2001). However, most of the work has focused on biosphere-atmosphere carbon exchange (Hollinger *et al.*, 2004; Baldocchi, 2008; Jung *et al.*, 2009; Stoy *et al.*, 2009) as well as on site-specific energy exchange studies (Admiral & Lafleur, 2007; Tanaka *et al.*, 2008; Peichl *et al.*, 2013). At the same time, fewer studies have concentrated on multi-site energy fluxes to infer biome wide or regional water and energy fluxes (Jung *et al.*, 2010; Wang & Dickson, 2012) aside from their relationship with CO_2 exchange (Hollinger *et al.*, 1999; Law *et al.*, 2002; Jung *et al.*, 2011). λE is estimated in eddy flux data from fluxes of water vapor, which are measured by using usually an infra red gas analyser (Foken, 2008). FLUXNET measurements have not been much used to estimate the energy balance of large regions, while micrometeorological problems, like energy balance closure (Wilson *et al.*, 2002; Foken, 2008; Barr *et al.*, 2012; Leuning *et al.*, 2012; Stoy *et al.*, 2013), EC footprint (Göckede *et al.*, 2008) and gap-filling (Falge *et al.*, 2001; Moffat *et al.*, 2007) have received much attention. In spite of these problems, EC technique is one of the best and least biased methods to measure water and energy fluxes at the ecosystem-scale.

The Penman–Monteith (PM) equation is one of the most widely used and accepted approaches to model λE (Katul *et al.*, 2012; Wang & Dickinson, 2012). The Penman Monteith method models explicitly the energy balance of an ecosystem: Net radiation is partitioned into latent heat flux (λE) and sensible heat flux depending on the surface (r_s) and aerodynamic resistances (r_a). It is widely used as a tool in agricultural related research (Allen, 1998) and has been used to analyze differences between boreal and temperate ecosystem (Blanken & Black, 2004; Zha *et al.*, 2010; Brümmer *et al.*, 2012). Recently, the approach has been extended by including various parameterizations to estimating surface resistance (r_s) (Grelle *et al.*, 1999; Valiantzas, 2006; Launiainen, 2010). In the simplest modifications, the aerodynamic (r_a) and surface resistance (r_s) are assumed to be constant on the daily level (Allen, 1998). Models with surface resistances that vary over time give better predictions of latent heat flux during a single day although models with constant canopy resistance give accurate predictions of λE over longer time spans (as e.g. daily or monthly) (Lecina *et al.*, 2003) However, stomatal regulation could become important, if the climate is changing and might change the values of surface resistance. The PM equation has previously been used successfully to estimate r_s in remote-sensing algorithms as well as in temperature-based λE models (Cleugh *et al.*, 2007; Mu *et al.*, 2011).

Lately, the interest concerning the importance and effects of phenology on ecosystem behavior has increased. There have been several studies investigating phenological effects on seasonal and annual carbon balance (Suni *et al.* 2003, Gea-Izquierdo *et al.*, 2010), bud burst (Richardson *et al.*, 2010), feedback mechanisms to the climate system (Richardson *et al.*, 2013) and spring onset (Richardson *et al.*, 2012). Richardson *et al.* (2012) conducted an analysis related to ecosystem-scale CO_2 exchange by using 14 different models in ten forested ecosystems. There are also some studies related to phenology and λE (e.g. Blanken *et al.*, 1997; Blanken & Black, 2004). However, the effect of delayed stomatal adaptation during the spring recovery to λE has been rarely estimated (Brümmer *et al.*, 2012).

In this article, flux and climate observations from FLUXNET are used to evaluate simulations of λE by using the PM equation. Boreal and arctic ecosystem types are investigated to determine how their modeled and measured λE depends on ecosystem type. Furthermore, a phenological model was used to investigate how the properties of the vegetation type affect λE. The hypothesis of the study was that different land cover classes differ in their λE and the way it depends on ecosystem properties and meteorological forcing.

Materials and methods

Study sites

Sixty-five sites representing the most common ecosystem types in the subboreal, boreal or arctic areas were selected from FLUXNET database (http://fluxnet.ornl.gov) for this study (Fig. 1; Table 1). Agricultural ecosystems were excluded from the analysis, because their annual cycle is mainly controlled by human activity like harvesting and seeding, fertilization or irrigation. Therefore, analysis was limited to natural ecosystems including forests that have been planted with native species after cuts. The selected sites were grouped based on the dominant plant functional type (PFT) into nine different categories. These were: (i) harvested or burnt areas temporarily void of trees (C), (ii) Douglas-fir forests (D), (iii) pine forests (P), (iv) spruce or fir dominated forests (S), (v) broadleaf deciduous forests (BD), (vi) larch forests (L), (vii) wetlands (W), (viii) tundra (T) and (ix) natural grasslands (G).

The attempt was to select available EC sites in the boreal and subboreal region, but to reject sites where measurements are restricted to summer periods with large gaps occur during the periods when λE are typically high. We acknowledged that the quality requirements were stricter for ecosystem types that are well represented in the database, while we had less stringent requirements for vegetation types that were not often measured. We thought that in these cases it might be important to increase the sample size of 'underrepresented ecosystems'. Exceptions were particularly made for tundra ecosystems, where data from winter months was very scarce. A complete site list with references, land type covers and climatological characteristics are presented in Table 1.

Data selection and estimation of missing measurements

For the data analysis, more than 400 EC site-years half-hourly of λE and meteorological data were checked for obvious measurement errors or reporting errors in units. Rather complete time series of seven meteorological variables were required for the estimation: air temperature (T_a), wind speed (u), friction velocity (u^*), global radiation (R_g), net radiation (R_n), air pressure (P_a) and relative humidity (RH). To avoid conditions when EC technique does not work properly, we removed periods with low turbulent mixing (u^* less than 0.1 m s^{-1}). Similar kind of data filtering criteria has been used previously in other studies (Alavi *et al.*, 2006; Wu *et al.*, 2010), but selected threshold value can be considered low for forests. It was selected mainly to ensure a similar kind of analysis for all ecosystems types (same u^* and kB^{-1}). Higher filtration criteria would have removed too much data from naturally open ecosystems (tundra, grasslands, wetlands, cut forests) and wintertime measurements from forests. Determination of optimal threshold value for each site or ecosystem type separately would have been hard and more or less subjective decision.

Thus, the most complete data series of half-hourly data were selected for the analysis and missing values for some of the meteorological data were estimated. First short gaps in T_a and RH (up to 4 h) were linearly interpolated (Amiro *et al.*, 2006). Longer gaps of these variables that could not be estimated by using mean diurnal variation (MDV) (Reichstein *et al.*, 2005) in a 14 days moving window, were filled by data recorded at the nearest weather station. This was done only for sites RU-Che, RU-Cok, RU-Ylr, RU-Ypf, RU-Sam, US-Atq, US-Brw, with distances varying from 1 to 50 km from the weather station. Weather station data are reported typically for every third or sixth hour and was interpolated to half-hourly values by using linear regression. Please note that the phenology model requires an air temperature history for the calculations related to delayed response of the vegetation to the increasing temperature during the spring [S & τ; see Eqn (4)]. It should also be noted that model parameter estimation was always done on nongap filled values of λE.

Missing periods in R_g data were estimated by using a linear regression relationships between photosynthetically active radiation (PPFD) as an independent variable. Estimated R_g was accepted only if the linear correlation coefficient between the estimated values and measured values exceeded 0.95, otherwise data were removed from estimation. Missing periods in R_n was estimated similarly between R_g and R_n and estimated values were accepted, if the linear correlation between estimated and independent variable exceeded 0.8. The theoretical relationship and conversion methods between radiation PPFD and short wave irradiance are reported in many studies (Weiss & Norman, 1985; Papaioannou *et al.*, 1993; Escobedo *et al.*, 2011), and instead of using constant relationships, parameters was estimated for each site separately by using site-specific measurements. Dry-foliage data were not used in the analysis, because all sites did not provided high quality precipitation data.

Model of latent heat exchange

The model parameters were estimated using the meteorological variables measured on site. The modeling was implemented using R software (R Core Team, 2013) by applying

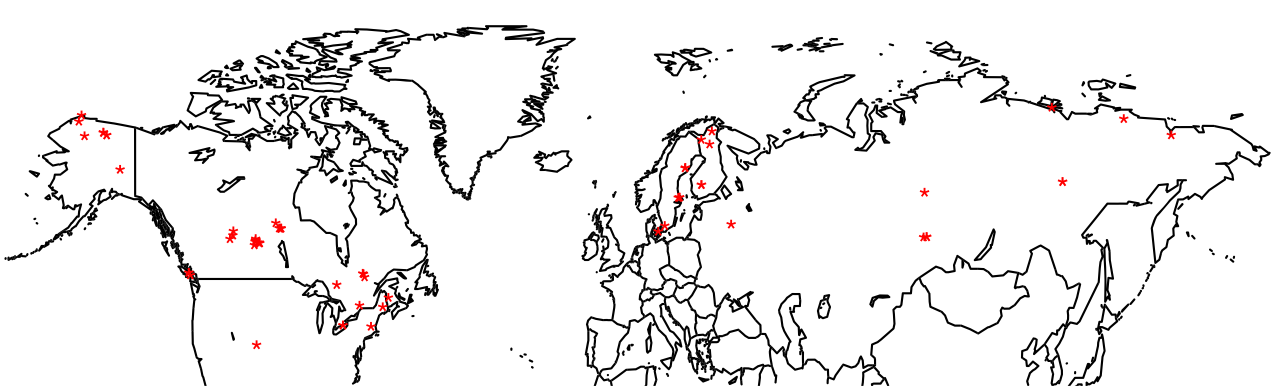

Fig. 1 Location of eddy covariance sites are marked with red star (*).

Table 1 Eddy covariance sites that were used in the study, coordinates, characteristics and site references

Sites			Coordinates		Characteristics		
Nr	Code	Name	Latitude	Longitude	IGBP	Forest type	Site reference
1	CA-Ca1	BC-Campbell River 1949 Douglas-fir	49.87	−125.33	ENF	Douglas-Fir	Krishnan *et al.*, 2009;
2	CA-Ca2	BC-Campbell River 2000 Douglas-fir	49.87	−125.29	ENF	Douglas-Fir	Krishnan *et al.*, 2009;
3	CA-Ca3	BC-Campbell River 1988 Douglas-fir	49.53	−124.9	ENF	Douglas-Fir	Krishnan *et al.*, 2009;
4	CA-Gro	ON-Groundhog River Mixedwood	48.22	−82.16	MF	Leaf	McCaughey *et al.*, 2006;
5	CA-Man	MB-Northern Old Black Spruce	55.88	−98.48	ENF	Spruce	Dunn *et al.*, 2007;
6	CA-Mer	ON-Mer Bleue Eastern Peatland	45.41	−75.52	WET	Wet	Lund *et al.*, 2009;
7	CA-Na1	NB-Nashwaak Lake 1 1967 Balsam Fir	46.47	−67.1	MF	Spruce	Yuan *et al.*, 2008;
8	CA-NS1	UCI 1850	55.88	−98.48	ENF	Spruce	Goulden *et al.*, 2011;
9	CA-NS2	UCI 1930	55.91	−98.52	ENF	Spruce	Goulden *et al.*, 2011;
10	CA-NS3	UCI-1964	55.91	−98.38	ENF	Spruce	Goulden *et al.*, 2011;
11	CA-NS4	UCI-1964 wet	55.91	−98.38	ENF	Spruce	Wang *et al.*, 2003;
12	CA-NS5	UCI 1981	55.86	−98.49	ENF	Spruce	Goulden *et al.*, 2011;
13	CA-NS6	UCI 1989	55.92	−98.96	ENF	Cut	Goulden *et al.*, 2011;
14	CA-NS7	UCI 1998	56.64	−99.95	ENF	Cut	Goulden *et al.*, 2011;
15	CA-Oas	SK-Old Aspen	53.63	−106.2	MF	Leaf	Black *et al.*, 1996;
16	CA-Obs	SK-Southern Old Black Spruce	53.99	−105.12	ENF	Spruce	Jarvis *et al.*, 1997;
17	CA-Ojp	SK-Old Jack Pine	53.92	−104.69	ENF	Pine	Griffis *et al.*, 2003; Zha *et al.*, 2010
18	CA-Qc2	QC-1975 Harvested Black Spruce	49.76	−74.57	MF	Cut	–
19	CA-Qcu	QC-2000 Harvested Black Spruce	-49.27	−74.04	ENF	Cut	Bergeron *et al.*, 2008;
20	CA-Qfo	QC-Eastern Old Black Spruce	49.69	−74.34	ENF	Spruce	Bergeron *et al.*, 2008;
21	CA-Sf1	SK-1977 Fire	54.49	−105.82	ENF	Pine	Mkhabela *et al.*, 2009;
22	CA-Sf2	SK-1997 Fire	54.25	−105.88	MF	Cut	Mkhabela *et al.*, 2009;
23	CA-Sf3	SK-1998 Fire	54.09	−106.01	ENF	Cut	Mkhabela *et al.*, 2009;
24	CA-Sj2	SK-2002 Jack Pine	53.94	−104.65	ENF	Cut	Coursolle *et al.*, 2006;
25	CA-Sj3	SK-1975 (Young) Jack Pine	53.88	−104.65	ENF	Pine	Margolis & Ryan, 1997;
26	CA-TPW	ON-Turkey Point 1974 White Pine	42.71	−80.35	MF	Pine	Peichl *et al.*, 2010;
27	CA-Tp4	ON-Turkey Point 1939 White Pine	42.71	−80.36	MF	Pine	Peichl *et al.*, 2010;
28	CA-Wp1	AB-Western Peatland	54.95	−112.47	MF	Wet	Flanagan & Syed, 2011;
29	CA-Wp2	AB-Western Peatland Poor Fen	55.54	−112.33	ENF	Wet	Adkinson *et al.*, 2011;.
30	CA-Wp3	AB-Western Peatland Rich Fen	54.47	−113.32	MF	Wet	Adkinson *et al.*, 2011;
31	DK-Sor	Soroe- Lille Bogeskov	55.49	11.64	DBF	Leaf	Pilegaard *et al.*, 2001, 2003;
32	FI-Hyy	Hyytiälä	61.85	24.3	ENF	Pine	Launiainen, 2010;
33	FI-Kaa	Kaamanen wetland	69.14	27.3	WET	Wet	Aurela *et al.*, 2004; Lund *et al.*, 2009;
34	FI-Lom	Lompolojänkkä	68	24.21	WET	Wet	Aurela *et al.*, 2009; Lohila *et al.*, 2010;
35	FI-Sii	Siikaneva	61.83	24.19	WET	Wet	Lund *et al.*, 2009;
36	FI-Sod	Sodankylä	67.36	26.64	ENF	Pine	Thum *et al.*, 2007;
37	RU-Che	Cherskii	68.61	161.34	OSH	Tundra	Corradi *et al.*, 2005; Merbold *et al.*, 2009;
38	RU-Cok	Chokurdakh/Kytalyk	70.83	147.49	OSH	Tundra	van Huissteden *et al.*, 2005;
39	RU-Fyo	Fedorovskoye wet spruce stand	56.46	32.92	ENF	Spruce	Kurbatova *et al.*,2008;
40	RU-Ha1	Ubs Nur-Hakasija-grassland	54.73	90	GRA	Grass	Belelli-Marchesini *et al.*, 2007a;
41	RU-Ha2	Ubs Nur-Hakasija-recovering grassland	54.77	89.96	GRA	Grass	Belelli-Marchesini, 2007b;
42	RU-Ha3	Ubs Nur-Hakasija-Site 3	54.7	89.08	GRA	Grass	Belelli-Marchesini, 2007b;
43	RU-Sam	Samoylov Island Lena Delta	72.37	126.5	OSH	Tundra	Boike *et al.*, 2013;

Table 1 (continued)

Sites			Coordinates		Characteristics		
Nr	Code	Name	Latitude	Longitude	IGBP	Forest type	Site reference
44	RU-Ylr	Yakutsk-Larch	62.26	129.62	DNF	Larch	Ohta *et al*., 2008;
45	RU-Ypf	Yakutsk-Pine	62.24	129.65	DNF	Pine	Hamada *et al*., 2004;
46	RU-Zot	Zotino	60.8	89.35	ENF	Pine	Tchebakova *et al*., 2002;
47	SE-Deg	Degero Stormyr	64.18	19.56	GRA	Wet	Lund *et al*., 2009;
48	SE-Faj	Fajemyr	56.27	13.55	WET	Wet	Lund *et al*., 2007;
49	SE-Fla	Flakaliden	64.11	19.46	ENF	Spruce	Lindroth *et al*., 2008;
50	SE-Nor	Norunda	60.09	17.48	ENF	Spruce	Lindroth *et al*., 1998;
51	SE-Sk1	Skyttorp young	60.13	17.92	ENF	Pine	-
52	SE-Sk2	Skyttorp	60.13	17.84	ENF	Pine	Gioli *et al*., 2004;
53	US-An1	Anaktuvuk River Severe Burn	68.99	−150.28	OSH	Tundra	Rocha & Shaver, 2011;
54	US-An2	Anaktuvuk River Moderate Burn	68.95	−150.21	OSH	Tundra	Rocha & Shaver, 2011;
55	US-An3	Anaktuvuk River Unburned	68.93	−150.27	OSH	Tundra	Rocha & Shaver, 2011;
56	US-Atq	Atqasuk	70.47	−157.41	GRA	Tundra	Lund *et al*., 2009;
57	US-Bn1	Delta Junction 1920 Control site	63.92	−145.38	ENF	Spruce	Liu *et al*., 2005;
58	US-Brw	Barrow	71.32	−156.63	SNO,BSV	Tundra	Walker *et al*., 2003;
59	US-Ha1	Harvard Forest EMS Tower (HFR1)	42.54	−72.17	MF	Leaf	Urbanski *et al*., 2007;
60	US-Ho1	Howland Forest (Main Tower)	45.2	−68.74	MF	Spruce	Hollinger *et al*., 2004;
61	US-Ich	Imnavait Creek Watershed Heath Tundra	68.61	−149.3	OSH	Tundra	Euskirchen *et al*., 2012;
62	US-ICs	Imnavait Creek Watershed Wet Sedge Tundra	68.61	−149.31	OSH	Tundra	Euskirchen *et al*., 2012;
63	US-Ict	Imnavait Creek Watershed Tussock Tundra	68.61	−149.3	OSH	Tundra	Euskirchen *et al*., 2012;
64	US-Ivo	Ivotuk	68.49	−155.75	OSH	Tundra	Epstein *et al*., 2004;
65	US-NR1	Niwot Ridge (LTER NWT1)	40.03	−105.55	ENF	Spruce	Hu *et al*., 2010;

nonlinear least squares regressions (using the nls-function of the statistics package with the nl2sol algorithm).

We estimated λE using the PM equation written as follows (Penman, 1948; Allen, 1998):

$$\lambda E = \frac{\Delta R_n + \rho_a c_p \delta_e r_a^{-1}}{\Delta + \gamma (r_s + r_a) r_a^{-1}} \quad (1)$$

where ρ_a is the air density (kg m^3), c_p is the specific heat of air (J kg^{-1} K^{-1}), Δ is the rate of change of saturation vapor pressure with air temperature (Pa K^{-1}) and γ is the psychrometric constant (66 Pa K^{-1}), r_s the surface resistance (s m^{-1}) and r_a the aerodynamic resistance (s m^{-1}). The latter was calculated from the EC data following the method used by Launiainen (2010):

$$r_a = \frac{u}{u_*^2} + \frac{\mathrm{kB}^{-1}}{u_*} \quad (2)$$

where kB^{-1} is the Stanton number (dimensionless). The excess resistance parameter kB^{-1} was set to the value of two (dimensionless) to estimate r_a in a similar way for all sites. This value is suggested to be representative for a wide range of vegetation types (Garratt, 1978), and has been found to be representative for forests (Verma, 1989; Launiainen, 2010). Among different studies various values for kB^{-1} has been used and its optimal value can vary between vegetation types as well as seasonally (Kustas *et al*., 1989; Wu *et al*., 2000; Barr *et al*., 2001; Zha *et al*., 2010). Although we used the same value of kB^{-1} for all sites, it has been reported to range from 1 to 12 (Shuttleworth & Wallace, 1985; Kustas *et al*., 1991; Troufleau *et al*., 1995).

Normally the PM equation includes the available energy flux (R_n–G–ΔS, where G is the soil heat flux and ΔS is the rate of heat storage in the canopy volume), whereas we have chosen to neglect G and ΔS since they are usually small compared to R_n particularly when using the equation on a daily basis (the two terms become small on a 24-h cycle). Based on the results of those studies that has been investigating EC energy balance closure problems, measurement errors of G and ΔS varies from 20 to 50% and the absolute flux gradient from 20 to 50 W m^{-2} (Foken, 2008). These components are small compared to Rn, λE and sensible heat flux (H) and their vertical and horizontal scales are limited to near ground level. Because these components were not widely reported for all ecosystem types present in the study, these terms were neglected from the estimation procedure and the decision to prioritize the wider coverage of different ecosystem types were made.

The surface resistance was estimated using a multiplicative model (Jarvis, 1976; Stewart, 1988) as follows:

$$r_s = f(P) f(\delta_e) f(R_g) \quad (3)$$

where $f(P)$, $f(\delta_e)$ and $f(R_g)$ are phenology, δ_e and R_g modifiers, respectively. The values of the modifiers vary between 0 and 1.

Table 2 Ecosystem specific calibrated model parameters

	Model parameters					
Vegetation types	θ (°C)	τ (d)	r_{SMax} (s m^{-1})	r_{SMin} (s m^{-1})	k_R (W m^{-2})	k_{VPD} (Pa)
Cut	13	25	79.2	22.4	14.3	282.8
Douglas-Fir	5	2	80.4	45.7	5.2	367.8
Grass	15	20	407.7	66.4	0.1	1372.1
Larch	6	22	75.5	13.2	87.1	220.0
Broadleaf deciduous	13	23	59.8	6.6	109.3	236.4
Pine	10	24	127.8	30.0	12.5	498.9
Spruce	12	15	71.3	25.5	41.8	473.8
Tundra	7	12	147.8	80.3	418.9	2700.7
Wet	7	11	232.3	90.1	12.2	4000.0

The phenology modifier which accounted for seasonal (i.e. summer and winter) are based on the work of Mäkelä *et al.* (2004) and Gea-Izquierdo *et al.* (2010) and is expressed as follows:

$$f(P) = r_{SMax} - 2\left(1 - \frac{1}{1+S(t)}\right)(r_{SMax} - r_{SMin}) \quad (4)$$

where r_{SMax} and r_{SMin} are the maximum and minimum stomatal resistances (s m^{-1}) and $S(t)$, a variable describing the phenological state of the plants, is calculated as follows:

$$S(t) = \min\left(\frac{\int_{t-\tau}^{t} T_a(t)dt}{\tau\theta}, 1\right), \quad (5)$$

where T_a is air temperature, θ (°C) is a parameter describing the long-term average temperature at which stomatal resistance reaches its minimum value, τ is the integration time delay of stomatal response in days. The phenological model describes the slow development of surface resistance to changes in temperature as it occurs during spring. It is a modification of the model of Gea-Izquierdo *et al.* (2010) that they used for the analysis of Gross Primary Production (GPP). The behavior of $S(t)$ as a function of τ and θ and T_a is shown in Fig. 2.

Surface resistance was also assumed to have a hyperbolic dependence on R_g (Wong *et al.*, 1979; Leuning, 1995) as follows:

$$f(R_g) = \frac{k_R + R_g}{(R_g + 5)} \quad (6)$$

where k_R is a parameter describing the sensitivity of surface resistance to global radiation. An offset of five W m^{-2} was added to R_g (in the denominator) to avoid frequent problems caused by occurrences of negative values of R_g and to constrain r_s surface resistance to finite values.

Finally, r_s was assumed to depend on δ_e as follows:

$$f(\delta_e) = \left(1 + \frac{\delta_e}{k_{VPD}}\right) \quad (7)$$

where k_{VPD} (kPa) is an empirically estimated parameter describing the sensitivity of stomatal conductace to δ_e. High values of k_{VPD} indicate a low stomatal sensitivity to VPD.

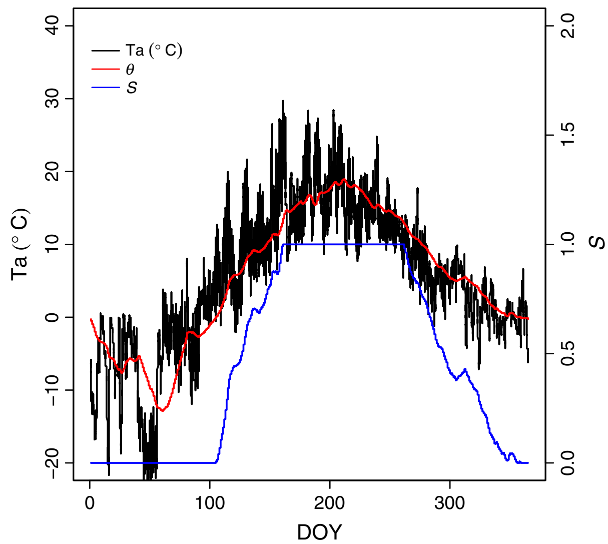

Fig. 2 Conceptual behavior of S as a function of θ and τ. The black line is the measured air temperature. The variable S (blue line) is calculated based on the running mean (blue line) of the measured air temperature (black line) and with delay (which depends on τ). S is saturated when it reaches the value 1 (on the right y-axes).

Statistical analysis

Parameter estimation was done using half-hourly values of r_s calculated by inverting Eqn (1) using nongapfilled λE, R_n, T_a, δ_e, u and u_* data. The values of the parameters k_R, k_{VPD}, r_{SMin}, r_{SMax}, θ and τ were estimated to maximize the fit of the model to measured λE data using ordinary least squares. Over all, two different parameter sets are estimated. Firstly, estimated parameter values for each site is provided separately and secondly, the estimated average parameters are provided for each vegetation type.

The values of the parameters k_R, k_{VPD}, r_{SMin} and r_{SMax} were estimated simultaneously. The parameters θ and τ, linked to the phenology of latent heat exchange, were estimated, iteratively. The values of θ and τ were first fixed and then the other parameters were estimated by using the nonlinear regression. The reported values are the combination of all parameters (including θ and τ), which minimizes the residual sum of squares. This was done for a grid with a density of 1 day (τ) and 1 °C (θ). The grid ranged from 1 to 30 days for τ and for 5–20 °C for θ. In rare cases where the use of the phenology model improved the fit of the model by less than 2%, θ and τ were set to 5 °C and 2 days, respectively.

To produce mean model parameters for each ecosystem type, all ecosystem specific data were concatenated and average ecosystem type parameters were estimated from this pooled data. Based on the parameters derived from this estimation, the λE values of different vegetation types were compared by using the ecosystem average model parameters for each vegetation type (r_{SMax}, r_{SMin}, k_R and k_{VPD}) and the meteorological data of the station Hyytiälä (FI-Hyy) for 2011. Hyytiälä was selected it represents somehow an 'average climate' in the dataset [mean annual air temperature 1961–1990 + 2.9 °C and precipitation 709 mm (Sevanto *et al.*, 2006)]. To compare the annual mean behavior of measured and modeled λE, site-specific data were aggregated (measured and modeled) over the whole data range as daily means (Table 3).

The goodness of the model fit was estimated by using the proportion of explained variance (PR^2), defined as:

$$PR^2 = 1 - \frac{\Sigma(y-\hat{y})^2}{\Sigma(y-\bar{y})^2}, \tag{8}$$

where y is the measured value of the variable in question, $\hat{y}$ is its predicted value and $\acute{y}$ its mean measured value. For a linear regression, this gives the same values as the traditional R^2.

Climatological and land cover data

To characterize the relations of vegetation characteristics to climate, long-term averages of climate variables were used. These were extracted from the Climatic Research Unit (CRU) gridded climatology (New *et al.*, 2002). This data have a spatial resolution of 10 min and the climate variables were gridded averages1960–2000. Averaged annual mean temperatures were in a good agreement with temperatures calculated from the available EC site data. Recorded T_a data from the EC sites could not directly be used, because from some sites data were available only for the summer time and some time series were quite short.

Leaf Area Index (LAI) and Normalized Difference Vegetation Index (NDVI) data are derived from the Moderate Resolution Imaging Spectroradiometer (MODIS) products [MOD13Q1 (18 days) & MOD15A2 (8 day)]. Grid size for LAI was 1 × 1 km and for NDVI 0.25 × 0.25 km from the center coordinates of the flux tower site. LAI and NDVI data are reported for July, which were assumed to be the time of maximum leaf area index at most sites.

Results

Site characteristics

Annual average T_a (as calculated from the climatological data) ranged between −10 to +8 °C, being lowest for tundra and highest for the Douglas-fir sites. Some of the most continental sites, Yakutsk-larch and pine sites (RU-Ylr and RU-Ypf) also had very low annual mean temperatures (−10 °C) (Fig. 3a). The mean annual precipitation was highest for the Douglas-fir sites (1600 mm a^{-1} CA-Ca1, CA-Ca2, CA-Ca3) and lowest for tundra sites (200 mm a^{-1} RU-Che, RU-Cok, US-Atq, US-An1, US-An2, US-An3, US-Brw, US-Ich, US-ICs, US-Ict, US-Ivo), while the mean precipitation for other vegetation types ranged between 500 and 600 mm a^{-1} (Fig. 3b). Mean annual T_a and precipitation were highly correlated (log (y) = $6.31e^{(0.0134x)}$ PR^2: 0.77 where y is mean annual precipitation and x is mean air temperature Fig. 3c).

Moderate Resolution Imaging Spectroradiometer derived mean summer LAI (using projected LAI) for most vegetation types in July, were around two and lowest summer time means were observed for grass, tundra and wetland sites (Fig. 3d). The highest LAI

Table 3 Statistical summary for the modeled ecosystem specific fit. RMSE is root-mean-square deviation, MM is measured mean

	Half an hour				Daily				Monthly			
Ecosystem	Bias	RMSE	MM	PR^2	Bias	RMSE	MM	PR^2	Bias	RMSE	MM	PR^2
Cut	−0.82	23.61	51.72	0.6	0.93	11.3	46.11	0.84	1.19	6.79	46.05	0.94
Douglas-fir	0.28	27.74	64.34	0.48	0.54	15.1	57.92	0.71	1.18	7.28	58.61	0.9
Grass	2.67	26.08	87.89	0.71	2.64	14.11	79.56	0.86	5.41	8.58	73.76	0.93
Broadleaf deciduous	−3.59	30.88	68.24	0.67	−0.38	15.44	65.64	0.85	−0.08	10.58	66.29	0.93
Pine	0.73	22.7	48.94	0.62	3.09	10.27	45.86	0.87	3.2	6.22	44.21	0.95
Spruce	−0.12	25.86	54.54	0.59	3.68	11.47	52.26	0.84	3.57	7.88	51.93	0.93
Tundra	6.19	24.96	53.75	0.52	5.81	14.21	36.82	0.61	4.69	8.28	27.24	0.83
Wet	1.51	23.09	67.1	0.76	3.22	11.94	60.22	0.88	3.76	8.39	61.08	0.95

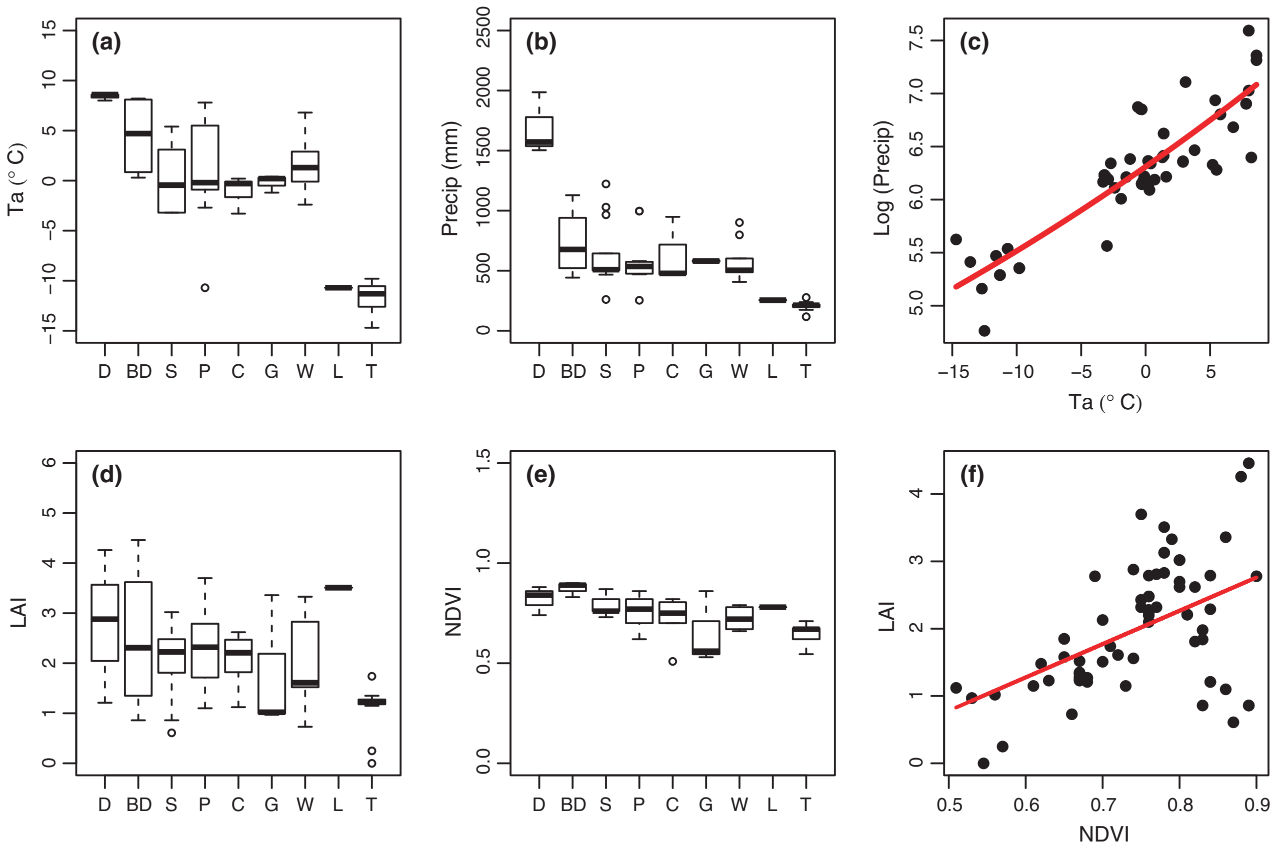

Fig. 3 Characteristic of the different vegetation types. (a) the variation in the mean annual air temperature (°C) (b) mean annual precipitation (mm) (c) logarithmic relationship of mean annual precipitation and air temperature log (y) = $6.31e^{(0.0134x)}$ PR^2: 0.77, (d) mean summer time LAI-index (e) Mean summer time NDVI, (f) regression between mean summer time LAI and NDVI index y = 4.9504x–1.6940 PR^2: 0.26. Results are presented in subpanels a, b, c and e by ecosystem type where, D, Douglas-fir forest; BD, broadleaf deciduous f.; S, spruce f.; P, pine f.; C, cut/open/burned f.; G, grassland; W, wetland; L, larch forest and T, tundra.

was observed in deciduous broadleaf, larch and Douglas-fir forests. The variation in NDVI and LAI was quite similar between ecosystem types (Fig. 3e). However, MODIS-derived NDVI as well as the LAI, were only weakly correlated with mean annual T_a ($y = 0.0081x + 0.7509$ $R^2 = 0.29$, where y is NDVI and x is T_a; $y = 0.0485x + 2.0669$ $R^2 = 0.10$, where y is LAI and x is air temperature). Also the correlation between NDVI and LAI was not strong ($y = 5.6x–2.71$; $R^2 = 0.31$ where y is LAI and x is NDVI) (Fig. 3f). The larch forest was the exception because, despite the low annual mean T_a and precipitation, summer time mean LAI and NDVI were almost as high as for the broadleaf-type forests (Fig. 3d and e).

Phenological model parameters

For the wetland- and tundra land cover types, the parameters indicating the saturation temperature to reach minimum value of r_s (θ) and the delay (τ) were smaller than for the forested sites. In other words, these ecosystems shifted from the winter to the summer state more rapidly and at lower temperatures. Among the forest sites, only the larch forest had a similar low temperature requirement. Usually forests reached summer resistance when θ varied between 10 and 13 °C with τ varying from 15 to 25 days (Table 2; Fig. 4a, b). The longest spring recovery period (as measured by τ and θ, were observed for grassland ecosystems. For these ecosystems, the values of θ were higher than for other ecosystems and values of τ were higher than for tundra and wetland ecosystems. Douglas-fir did not show any seasonal pattern for r_s, and the parameter values for the phenology model are not reliable since the difference between parameters describing wintertime resistance (r_{SMax}), and summertime resistance (r_{SMin}) was small (Table 2).

r_{SMax}. The calculated maximum canopy resistance parameters r_{SMax} varied between 100 and 250 s m^{-1} for all vegetation types (r_{SMax} in Fig. 4c). Winter values of r_s values were clearly higher than the summer values in

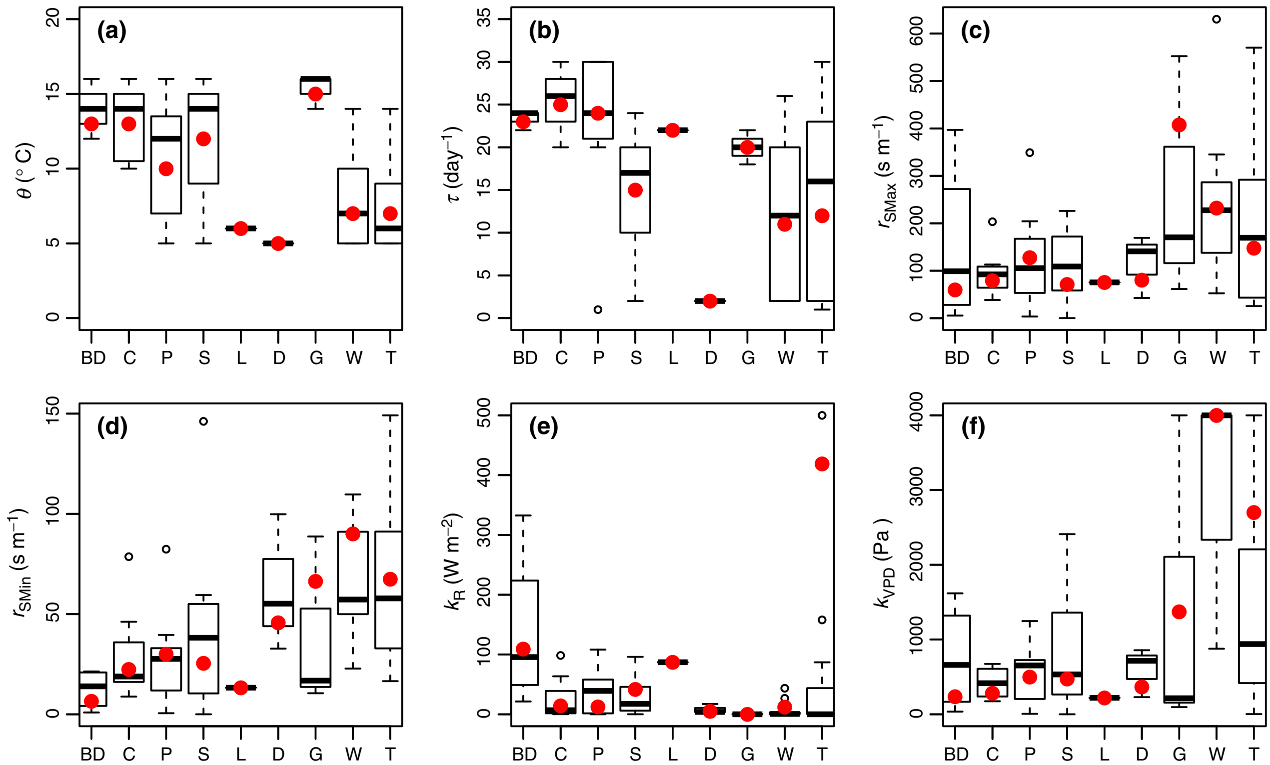

Fig. 4 Distribution of model parameters θ (°C) (a), τ (days) (b) maximum resistance r_{SMax} (c), minimum resistance r_{SMin} (d) sensitivity global shortwave radiation k_R (e) and sensitivity to rapid VPD changes k_{VPD} (f). Results are presented in all subpanels according to ecosystem types where, BD, broadleaf deciduous forest; C, cut/open/burned f.; P, pine f.; S, spruce f.; L, larch f.; D, Douglas-fir f.; G, grassland; W, wetland and T, tundra. Red points are model parameters that are calibrated against the all ecosystem type data and represent values estimated for all sites of an ecosystem type. Heavy black line of the box-and-wisker plot shows the arithmetic mean, thin black line 25% and 75% quartiles, and wisker lines (or single points) minimum and maximum values of the data. Red points are model parameters that are calibrated against the all ecosystem type data.

all ecosystems excluding Douglas-fir. The variation in wintertime r_s parameters within grassland, broadleaf deciduous forest and wetland ecosystems was large, while the variation for evergreen coniferous forest ecosystems was smaller (Fig. 4c).

r_{SMin}. The highest mean values of r_{SMin} were observed for Douglas-fir, grassland, tundra and wetland (Fig. 4d). For coniferous forests, the values of r_{SMin} were about half of the values for deciduous forests. Broadleaf deciduous forests had the smallest values of summer time r_s followed by the other forest ecosystems with exception of Douglas-fir. Douglas-fir had high values of r_s. In general, wetlands and tundra ecosystems had higher values of r_s than forests.

k_R. The mean values of k_R, which describes the sensitivity of the surface resistance to R_g were small for all sites, typically less than 100 W m^{-2}. There was no clear relationship of k_R with vegetation type or climatic characteristics. The largest variation in k_R was observed for the broadleaved deciduous forest vegetation type (Fig. 4e).

k_{VPD}. High values of k_{VPD} indicate that r_s changes slowly with increasing $_e$, while low values indicate a rapid reduction in r_s when $_e$ increases. Low values of k_{VPD} can be interpreted that stomatal resistance (r_s) is sensitive to vapor pressure deficit (δ_e). Values of k_{VPD} were higher (>500 Pa) for sites where freely evaporating water is present, and low (<500 Pa) for sites where the evaporative flux is governed by largely by stomatal regulation. The values were highest for the grass, tundra and wetland-types (Fig. 4f).

Mean parameters for ecosystem types

Modeled mean parameters (red dots in Fig. 4; Table 2) for different ecosystem types were mainly within the variation range and close to arithmetic means from the site-specific estimation (black lines in Fig. 4). r_{SMax}

was slightly lower for all ecosystem types than the calculated mean, grassland and pine excluded. r_{SMin} was higher than the mean for grassland, tundra and wetland, while values for Douglas-fir, broadleaf deciduous and spruce were slightly lower. For all ecosystems types, k_R values were similar to the mean values and only for tundra-type the parameter was clearly higher. The modeled k_{VPD} parameter was similar to the mean or slightly lower for all other sites, but higher for grassland and tundra.

Aerodynamic resistance (r_a)

Aerodynamic resistance was calculated from the recorded EC data based on Eqn (2). Typically r_a was smaller for forests than for open ecosystems (Fig. 5a). In most forest ecosystems, median values of r_a from half-hourly data were less than 50 s m^{-1}, Douglas-fir excluded. For grassland, tundra and wetlands that are usually more open ecosystems than forests, r_a varied typically from 50 to 150 (s m^{-1}) (Fig. 5a). r_a values derived from estimation where ecosystem specific data were pooled, (red dots) were quite similar to calculated averages for ecosystems (black horizontal lines in Fig. 5a).

Surface resistance (r_s)

Surface resistance was calculated according to Eqns (3-7) and the overall pattern of ecosystem median values was opposite to r_a. Usually, those systems that had low r_a, had higher r_s, and those with high r_a, had low r_s (Fig. 5b). The highest median values of r_s, calculated from half-hourly data, were found for broadleaf deciduous and larch, followed by evergreen needle leaf and cut forests. For wetlands, grasslands and tundra r_s was typically lower than for forest ecosystems. r_s from pooled ecosystem calibration were quite similar to calculated means (red dots in Fig. 5b), but lower for broadleaf deciduous forests. For wetlands and tundra, estimated values from pooled data were higher than the calculated means (Fig. 5b).

Partitioning total resistance between rs and ra

Total resistance was calculated as the sum of r_a and r_s. Forests have typically higher r_s than ecosystems with short vegetation, where aerodynamic resistance controls the total resistance (Fig. 5c). This can be seen from Fig. 5c where r_s in all forest ecosystems contributes clearly more than 50% of the total resistance (r_s + r_a), while for other ecosystems this proportion is typically less. The range in of the ratio of r_s to $r_s + r_a$ varies mostly in cut forests, wetland and tundra. This indicates the heterogeneity of these ecosystem types. For example, the length of the roughness elements (height of the vegetation) is not similar in different kind of cut forests, wetlands or tundra, while in mature forests and grasslands the variation is smaller. The importance of r_s calculated based on pooled data is within the range of the ecosystem specific variation. However, in the pooled data the importance of r_s was larger for wetlands and tundra (Fig. 5c).

Fit of the model

The proportion of explained variance (PR^2) between measured and predicted λE for half-hourly values var-

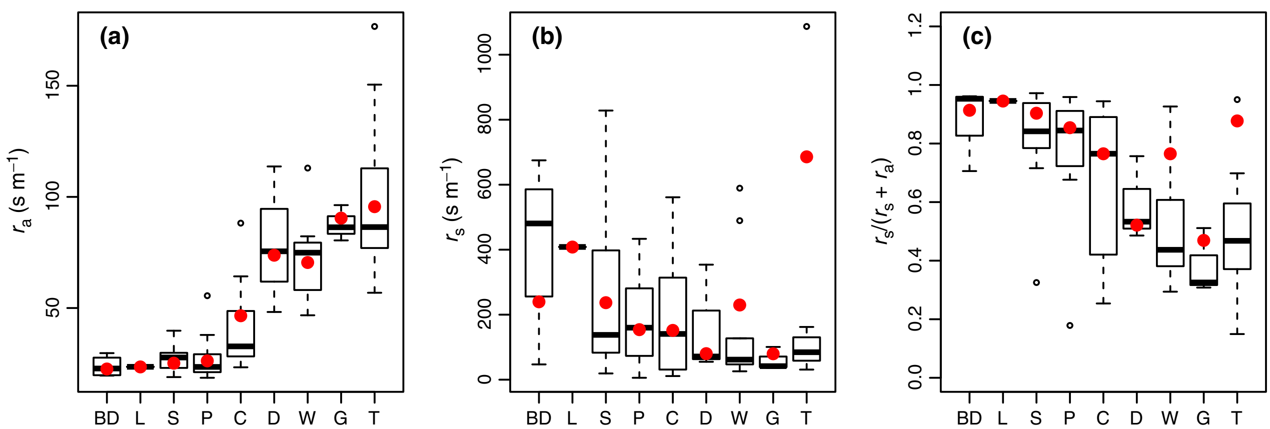

Fig. 5 Distribution of calculated median aerodynamic resistance (r_a) from half an hour data (a), distribution of calculated median surface resistance (r_s) from half an hour data (b) and proportion of total resistance accounted for r_s (i.e., the ratio of r_s to r_s + r_a) (c) based on the data presented in panels a and b. Results are presented in all subpanels according to ecosystem types where, BD, broadleaf deciduous forest, C, cut/open/burned forest; P, pine forest; S, spruce forest; L, larch forest; D, Douglas-fir forest; G, grassland; W, wetland and T, tundra.

ied from 0.4 to 0.84 among sites. The mean PR^2 value was 0.65 ± 0.11 (mean ± SD). When we compared daily mean λE values to daily averages of the modeled data the PR^2 varied from 0.33 (CA-Man) to 0.92 (CA-NS5) with a mean of 0.76 ± 0.11, and for monthly aggregation from 0.58 (RU-Cok) to 0.99 (RU-Ha1) with a mean 0.90 ± 0.07 (Table 3; Fig. 6). All model and statistical parameters for sites, as well as, ecosystem types are reported in S1.

Fits of the model based on the ecosystem type specific estimation, were slightly lower than the arithmetic mean from the site-specific calibration (red dots in Fig. 6a). However, for daily and monthly time steps, the fit was generally better than the arithmetic mean from the site-specific estimation (red dots in Fig. 6b and c). This was due to the increase in variance of the data when all the data for an ecosystem is pooled, and not actually due to a better fit of the model.

The aggregated daily mean values over the whole data range showed that the yearly patterns of measured and modeled λE in all ecosystem types were similar and indicate a good fit over all of the year (examples provided in Fig. 7).

Vegetation differences in λE

There was a strong relationship [$92.16e^{(0.0418x)}$, $P < 0.05$, $R^2 = 0.99$] between ecosystem type specific model parameters r_{SMin} and k_{VPD} calibrated against the pooled data (Fig. 8). In this regression, the small r_{SMin} indicates low summer time resistance that typically leads to higher λE flux. Like it can be seen from the Fig. 5c, r_s mainly controls λE in forest ecosystems. Forests seem also to be more sensitive to VPD changes (Fig. 8). Ecosystems that have values of r_{SMin} greater than 500 s m^{-1} (grasslands, wetlands and tundra), are not sensitive to VPD changes, but have lower value of r_s than most forests.

To compare the differences between ecosystems, the ecosystem specific λE flux was simulated by using mean ecosystem parameters and meteorological variables from site FI-Hyy. Even with identical levels of meteorological forcing differences between ecosystems were observed. The proportion of simulated λE of net radiation varied between ecosystems from 39% in broadleaf deciduous forest to 16% in tundra (Fig. 9).

Discussion

This study presents a comprehensive analysis of λE for different vegetation types of the northern temperate, boreal and arctic vegetation zones. The boreal and arctic zones are, by no means homogenous, but a mixture of different land cover types that are determined by the proportion of wetlands and frequency of disturbances (Bonan, 2008a,b). This study presents a new quantitation of energy exchange of different land cover types based on the data of 65 FLUXNET stations. It is demonstrated that these land cover types differ in their energy exchange and their response of surface resistance to the environment. The PM equation gave an adequate description of the λE for all vegetation types, however, the r_s parameters and the response of r_s to the environment differed between sites. Furthermore, phenological effects were important since wintertime and summer time resistances were different for all sites, except Douglas-fir.

The resistances, r_a and r_s, govern λE between vegetated surface and atmosphere. The resistances estimated for different ecosystem types are within the range of the reported variation in boreal ecosystems (Baldocchi *et al.*, 2000; Eugster *et al.*, 2000). Baldocchi *et al.* (2000) and Eugster *et al.* (2000) reported that total

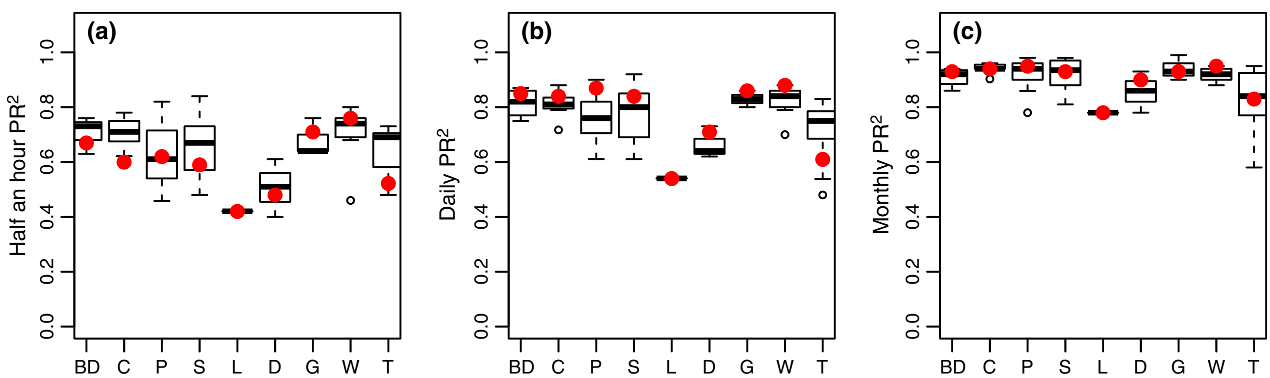

Fig. 6 Proportion of explained variance (PR^2) for 0.5 h (a), daily (b) and monthly (c) time span. Results are presented in all subpanels according to ecosystem types where, BD, broadleaf deciduous forest; C, cut/open/burned f.; P, pine f.; S, spruce f.; L, larch f.; D, Douglas-fir f.; G, grassland; W, wetland and T, tundra. Red points are PR^2 values from pooled estimation based on the ecosystem specific model parameters presented in Fig. 4.

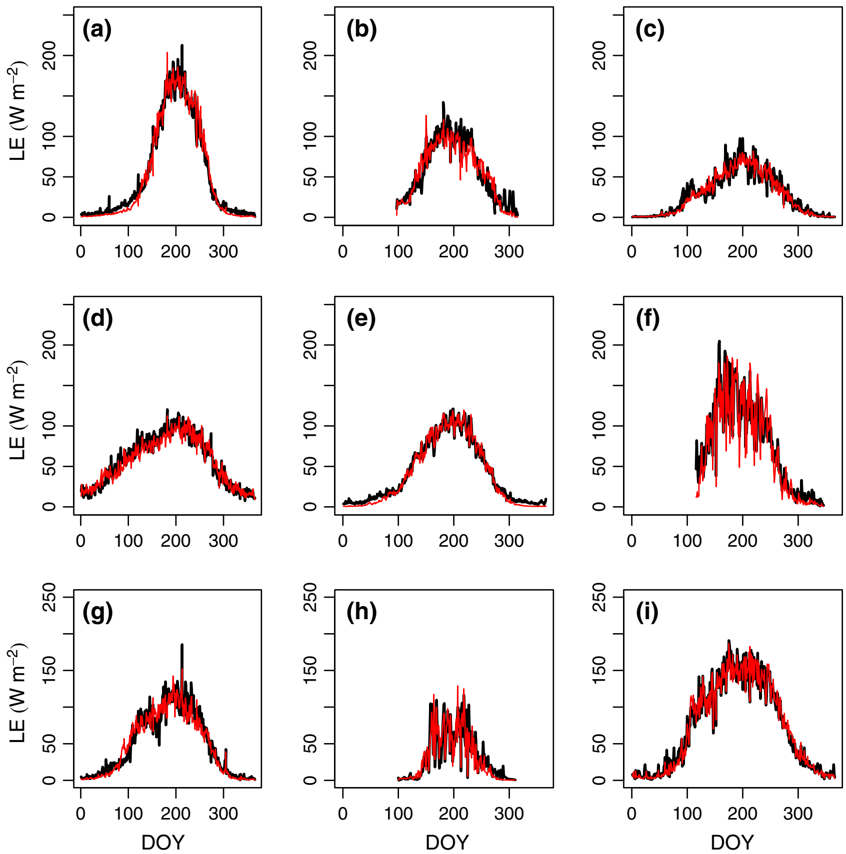

Fig. 7 Aggregated annual measured and predicted λE for different vegetation types over the data range used in the estimation. The black line is the mean daily λE and the red line represents modeled daily values. Subpanels represent data and fit of the model for following sites a: CA-Oas PR^2 0.98, b: RU-Ylr PR^2 0.85, c: CA-Sj2 PR^2 0.92, d: CA-Ca1 PR^2 0.93, e: FI-Hyy PR^2 0.98, f: RU-Ha1 PR^2 0.91, g: RU-Fyo PR^2 0.94, h: RU-Che PR^2 0.83, i: CA-Mer PR^2 0.98. Ecosystem types that sites are represented are (a) broadleaf deciduous forest, (b) larch forest, (c) cut forest, (d) Douglas-fir forest, (e) pine forest, (f) grassland, (g) spruce forest, (h) tundra, (i) wetland.

resistance in boreal ecosystems varies between 20 and 1500 s m^{-1}. In this study, we found that when the calculated median r_s exceeds 500 s m^{-1} in half-hourly data, the ratio of r_s to the total resistance is typically greater than 0.7. This suggests that in all these ecosystems r_s is the most important vegetation characteristics controlling λE. The range of the variation in the r_s model parameters was large also within the ecosystem types. Summer minimum resistance values (r_{SMin}) and the VPD sensitivity of the stomata (k_{VPD}) for different sites were strongly correlated (see Fig. 8). In this regression, broadleaf deciduous forest has the smallest r_{SMin}, followed by the other young and mature forest types, while grassland, tundra and wetland-type ecosystems have significantly higher r_{SMin} and seem not to be sensitive to changes in VPD. The observation of this study is consistent with previous findings (Kelliher *et al.*, 1995; Baldocchi & Vogel, 1997) and suggest that evergreen needle leaf forests have higher values of r_s than deciduous broadleaf stands.

Based on the findings of this study, λE in wetlands and tundra ecosystems occurs often from open water surface or the ground, while stomata largely control the λE of forests. The highest values for r_s were observed in tundra and wetland ecosystems. In both ecosystems types, mosses are very common or in some cases, the dominant vegetation cover. λE from feather moss, *Sphagnum* species and lichen are not similar to vascular plants due to the difference in physiological structure. Brown *et al.* (2010) reported that feather moss has higher resistance to λE than Sphagnum species, and Kettridge *et al.* (2013) showed that a higher tree density in wetlands affects λE.

The fit of the model was fair for half-hourly time periods (PR^2 around 0.6 for most ecosystem types) and the model was able to capture variation in all ecosystem types. Used radiation and flux data in the estimation was not corrected for the energy balance closure or other potential errors. Energy balance closure calculations were also not possible for some of the tundra sites

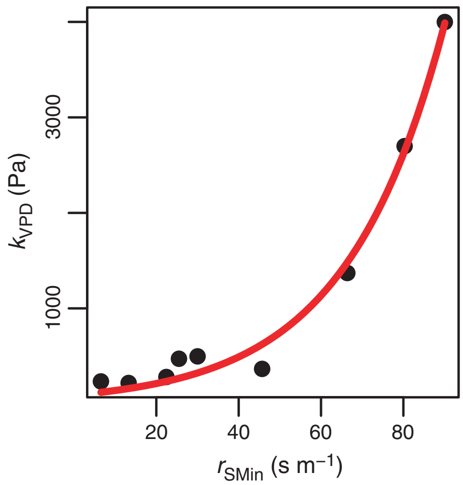

Fig. 8 Relationship between modeled ecosystem type specific parameters r_{SMin} and k_{VPD} $y = 92.16e^{(0.0418x)}$ PR^2 0.98. The order of dots from right to left with increasing r_{SMin} and k_{VPD} is broadleaf deciduous forest, larch forest, cut/open/burned forest, spruce forest, pine forest, Douglas-fir forest, grassland, tundra and wetland.

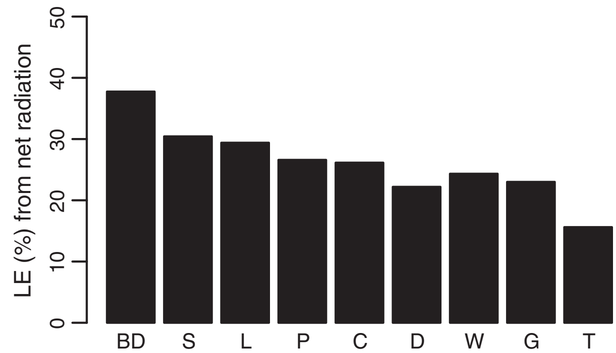

Fig. 9 Proportion (%) of annual net radiation (R_n) accounted for by of λE based on the parameter values estimated for each ecosystem type. Meteorological data from station FI-Hyy were used in the simulations. Results are presented according to ecosystem types where, BD, broadleaf deciduous forest; C, cut/open/burned forest; P, pine forest; S, spruce forest; L, larch forest; D, Douglas-fir forest; G, grassland; W, wetland and T, tundra.

where ground heat flux was not measured and eddy flux data for the whole year was not available. The mean PR^2 values of this study, were similar to values usually reported for carbon fluxes in similar ecosystems (Gea-Izquierdo *et al*., 2010). It is notable that the model performance was less than average for the Douglas-fir stands in both studies (this study and Gea-Izquierdo *et al*., 2010). While the explanatory power of the models was quite high, parameter values varied within and between vegetation types. Some of the variation in the parameters within a vegetation type can be explained by differences in the functioning of ecosystems on different sites, but some can be attributed to cross-correlation of parameters that increase the errors of the estimated parameter values (e.g. Gea-Izquierdo *et al*., 2010). Aside from the Douglas-fir sites the fit was also poor for some tundra sites.

The reasons for the lack of fit to Douglas-fir is ignored, because this ecosystem have not responded well either to earlier attempt to use phenological models. However, it can be considered that in tundra ecosystems some of the assumptions of the PM equation are not realized. Tundra ecosystems have a sparse vegetation cover and the melting of the active layer may induce a large heat sink (Rouse, 1984). Therefore, it is likely that the plant canopy is not warming as expected by the PM equation and the assumptions are violated in tundra ecosystems where the difference between R_n and soil heat flux might be necessary in estimating the available energy flux. For some sites, it is estimated that soil heat flux might account up to 30% of R_n (Rouse, 1984; Boike *et al*., 2008). This is particularly true since in some of our tundra sites a thin layer that overlays permafrost and heats up is used primarily to melt ice (Boike *et al*., 2008; Langer *et al*., 2011). Also, the evaporation in some tundra ecosystems seems to depend on precipitation since it changes the area covered by open water surfaces in these wet ecosystems (Boike *et al*., 2008).

Comparison of the simulated λE rates for different land cover types using climate data of the FI-Hyy site shows that λE and its sensitivity to environmental factors differs between land cover types. At identical values of R_n, u_* and u, λE was usually higher for forested sites than for the other sites, including wetlands. This is probably due to their larger transpiring leaf area. The highest values of λE were found for deciduous forests, followed by larch forests and fir or spruce forests. This is in agreement with the previous case studies that suggest that λE from deciduous leaf forest can be from 50 to 90% of the annual precipitation (Baldocchi *et al*., 2000; Chapin *et al*., 2000; Blanken *et al*., 2001) and r_s of evergreen conifers can be twice as large as that of deciduous broadleaf forests (Eugster *et al*., 2000). The simulated λE of short vegetation sites, grassland and tundra was less than for forests. The real difference is probably even larger since r_a tends to be larger for short vegetation sites. For example Nordbo *et al*. (2011) found that λE from the Hyytiälä pine forest exceeded the λE of a nearby lake, because the forest was better coupled to the atmosphere, i.e. the forest had a lower r_a.

The selected model for this study may also be criticized since it does not include drought in the soil. Although, several studies have shown the connection between soil moisture, LAI and λE (Barr *et al*., 2007;

Granier *et al.*, 2007), their relationship can be inconsistent and complex in different ecosystems (Eugster *et al.*, 2000). Typically conifers are less sensitive to drought than deciduous broadleaf trees (Lagergren & Lindroth, 2002; Bernier *et al.*, 2006; Kljun *et al.*, 2006). Because all sites did not provided both soil moisture and precipitation data, the effect of drought to λE it is neglected from this study. Previous studies have shown that the effect of drought can be hard to capture even with detailed models (Duursma *et al.*, 2008). Based on the analysis of the selected sites and data in this study, a special need to estimate model parameters separately was not found. The fit of our model is good without taking into account the possible drought effect throughout the season, which may indicate that drought in the northern ecosystems is not very important in boreal and arctic ecosystem.

There is also a large difference in parameters of the λE model between summer and winter periods for all ecosystem types except coastal Douglas-fir. The approach of this study to explain the seasonal variation in r_s is phenomenological and that the model describes different processes, like physiological changes of evergreens, snow melt and leaf growth for different land cover types. A similar approach has been used previously to predict GPP and explains well the differences between different seasons in the r_s model parameters (Berninger *et al.*, 1996; Mäkelä *et al.*, 2004; Mäkelä *et al.*, 2006).

The λE of deciduous broad leaf forests should depend largely on the expansion of leaf area (Blanken *et al.*, 1997). A shift from winter to summer values of r_s is expected when the forest starts to leaf out and GPP starts to increase. Leafing out of trees has traditionally been predicted using accumulated temperature models (Raulier & Bernier, 2000) and the temperature sum required partially depends on the genetic origin of the trees, but is mostly driven by the accumulation of cold days prior to warming. Baldocchi *et al.* (2005) used successfully an approach based on running averages of temperatures to predict the date when NEE equals 0 in northern deciduous broadleaf forests. We did not use the same approach as Baldocchi *et al.* (2005), since we have focused mainly on evergreen forests, where the approach does not apply. Instead, our approach emphasizes a gradual transition from winter to summer states in most common ecosystem types in boreal and arctic regions.

For evergreen conifers, it can be argued that the pronounced seasonal cycle we usually observe is caused by stomatal closure in the winter (Wieser, 2000) and to some extent by higher energy requirements when energy is used to melt snow rather than to evaporate water. Differences between winter and summer gas exchange are relatively well documented for photosynthetic capacity and attributed to photosynthetic down regulation (Suni *et al.*, 2003; Mäkelä *et al.*, 2004, 2008; Kolari *et al.*, 2007; Gea-Izquierdo *et al.*, 2010). Although, this approach has been used less for λE; there is evidence that stomatal resistance increase during the winter periods (Wieser, 2000; Sevanto *et al.*, 2006). The values of the time interval required for the recovery of transpiration (indicated by the parameter τ) were slightly higher than previously reported values related to the delayed photosynthesis using a large part of this data set (Gea-Izquierdo *et al.*, 2010). In this study, we observed values of the delay (τ) ranging from 2 to 30 days in different conifer forests. We think that the development of the LAI of the understory or other factors may play a role in determining the value of τ. Also Brümmer *et al.* (2012) reported clearly longer values for the delays in λE than for the photosynthesis thus the approach was more statistical than in this study and was done by using normalized cross-correlation coefficients (NCCC) to evaluate the lag of evapotranspiration behind R_n. The results of Brümmer *et al.* (2012) support the findings of this study that the delay on average is smaller in wetland and tundra ecosystems while from some ecosystems (Douglas-fir) or some sites it cannot be detected. However, without a comprehensive analysis of the links in the recovery of photosynthesis and evapotranspiration the linkages of down regulation recovery of GPP and of evapotranspiration after the winter remain speculative even if previous studies have indicate their potential relevance (Running, 1980; Grace, 1990).

At cut forest sites, the ecosystem is to some degree disturbed and consists of a natural mosaic of young trees, grass, shrubs and mosses. After a clear-cut, λE from the tree canopy ceases and λE from the ground vegetation increases. However, the disturbance does not necessarily decrease λE significantly (Vesala *et al.*, 2005; Jassal *et al.*, 2009). Increased light intensity in undergrowth increases photosynthesis and through that λE from vegetation and undergrowth and shrubs might be mainly accountable to λE (Baldocchi *et al.*, 2000; Rouse, 2000). Kelliher *et al.* (1998) reported that the understory might contribute between 30% and 92% (mean 54%) of the daily λE even in a mature pine forest and Blanken *et al.* (1997) that hazelnut understory transpiration exceeded 25% of total stand evapotranspiration in a mature aspen forest during the summer months.

Vesala *et al.* (2005) reported that thinning of a pine forest in the southern part of Finland did not change fluxes of water or carbon within the detection limits, but affected the physical properties of the canopy like wind speed normalized by the friction velocity. Altogether, it is not clear how leaf area, u_* and water use of trees interact. Intermediate disturbances of ecosystems do therefore not necessarily decrease fluxes of λE while the effect has been reported to be significant for the carbon balance in a boreal forest (Bergeron *et al.*, 2008). Indeed studies of water fluxes after thinning or other intermediate-severity disturbances show inconsistently either increases (Lagergren *et al.*, 2008) no changes (Vesala *et al.*, 2005) or small decreases in λE (Dore *et al.*, 2012).

For tundra and wetlands the interpretation of our temperature-based model for phenology is not very clear because mosses are typically the dominant plant functional type in these ecosystems. Therefore, the concept of surface resistance can be disputed and it is not as clear as in forests, where it is controlled by the stomata. In these systems, high r_{SMax} values are partly artificial, because stomatal resistance should not be important while the site is mainly snow covered, although evapotranspiration is still occurring through evaporation from the snow surface and sublimation.

Altogether, the temperature-based approach was useful, although for some ecosystems like tundra, it might be necessary to take into account also the soil heat flux. It seems that the approaches for GPP modeling by Gea-Izquierdo *et al.* (2010) for conifers and the approach of Baldocchi *et al.* (2005) for deciduous vegetation indicate that there are different environmental factors governing the recovery of the canopy. These phenological aspects should be explored in future modeling exercises at a more detailed scale. However, the phenomenological scheme worked quite well for large areas.

The relatively large variation in both site and ecosystem type specific k_{R} and k_{VPD} parameters suggests that the sensitivity of stomatal resistance to irradiance and VPD varies between ecosystem types but also between different sites covered by the same ecosystem type. The estimated k_R were smaller than we would have expected from physiological measurements of stomatal responses to irradiance (e.g. Gea-Izquierdo *et al.*, 2010). The estimated k_R values were usually small for deciduous forests ecosystems and tundra. The larger variation in k_{VPD} suggests that within grassland, tundra and wetland land cover types different ecosystems can have different sensitivities of r_s to δ_e (Fig. 4). Sites that have high $k_{\mathrm{VPD},}$ usually suffer less from water stress and their stomatal resistance is not sensitive to VPD. In the ecosystem type pooled estimation, the mean k_{VPD} values for tundra and wetlands were much higher than for forests where the r_s is expected to be the dominant term governing the water vapor flux. For some tundra- and wetland-type sites the summer resistance and sensitivity to VPD was higher than for other ecosystems.

The analysis suggests that there are large differences in the surface and aerodynamic resistances between different vegetation types in the boreal and arctic biomes (Fig. 5, Fig. 9). Surface resistance seems to regulate λE over the year in larch, most deciduous, pine and spruce forest, while the role of aerodynamic resistance is significant in clear-cut and burnt sites, tundra and wetland ecosystems.

Boreal landscapes are, from a standpoint of energy exchange, by no means homogenous and there are large differences in λE between different ecosystem types. The used approach led to relatively good estimates of latent heat exchange for these land cover types. Differences in surface resistance between the summer and winter periods are large, also for evergreen conifers, and might be important for the estimation of winter- and spring time latent heat exchange. The results suggest that the accuracy of regional energy exchange estimates will be vastly improved if the significance of stomatal regulation and phenology in different vegetation types is explicitly addressed.

Acknowledgements

This research was funded by the Nordic Center of Excellence CRAICC (Cryosphere-atmosphere interactions in a changing Arctic climate), Center of Excellence (project numbers 1118615, ICOS 271878 and ICOS-Finland 281255, ICOS-ERIC 281250 and EU through projects GHG-Europe and InGOS.

We are grateful from the possibility to utilized resources and data that are funded by Fluxnet-Canada, AmeriFlux and US National Science Foundation. The Fluxnet-Canada Research network was funded by the Canadian Foundation for Climate and Atmospheric Sciences (CFCAS), the Natural Sciences and Engineering Research Council (NSERC) of Canada, BIOCAP Canada, Natural Resources Canada and Environment Canada. The Canadian Carbon Program (CCP) was funded by CFCAS, BIOCAP Canada, Natural Resources Canada and Environment Canada. Additional support for both networks was provided by various provincial agencies and industry collaborators: Ministry of Environment (Ontario), Forestry Research Parnership (Canada) and Forestry Canada. The NOBS-MB site also received support from NASA (NAG5-11154 and NASA NNG05GA76G). We also thank TCOS-Siberia that enabled data collection in some Russian flux-towers as well as Helmholtz Association (Helmholtz Young Investigators Group, grant VH-NG-821) that funded the work of Torsten Sachs. We also thank FLUX-Asia for providing data for this study.

We also thank personally the following site PI's: Alan Barr, Allison Dunn, Brian Amiro, Charles Bourque, David Hollinger, Corinna Rebmann, Eugenie Euskirchen, Gaius Shaver, Hank Margolis, Harry McCaughey, J. William Munger, James Randerson, Lawrence Flanagan, Lise Soerensen, M. Martin Heimann, Mats Nilsson, Mike Goulden, Nigel Roulet, Peter Blanken and Riccardo Valentini and as well as all other persons who are not mentioned here, but has helped to produce data utilized in this study.

References

Adkinson AC, Syed KH, Flanagan LB (2011) Contrasting responses of growing season ecosystem CO_2 exchange to variation in temperature and water table depth in two peatlands in northern Alberta, Canada. *Journal of Geophysical Research*, **116**, 1–17.

Admiral SW, Lafleur PM (2007) Modelling of latent heat partitioning at a bog peatland. *Agricultural and Forest Meteorology*, **144**, 213–229.

Alavi N, Warland JS, Berg AA (2006) Filling gaps in evapotranspiration measurements for water budget studies: evaluation of a Kalman filtering approach. *Agricultural and Forest Meteorology*, **141**, 57–66.

Allen RG (1998) Crop Evapotranspiration (guidelines for computing crop water requirements). *FAO Irrigation and Drainage Paper*, **56**, 1–296.

Amiro B, Barr A, Black T *et al.* (2006) Carbon, energy and water fluxes at mature and disturbed forest sites, Saskatchewan, Canada. *Agricultural and Forest Meteorology*, **136**, 237–251.

Aubinet M, Grelle A, Ibrom A *et al.* (2000) Estimates of the annual net carbon and water exchange of forests: the EUROFLUX methodology. *Advances in Ecological. Research*, **30**, 113–175.

Aurela M, Laurila T, Tuovinen JP (2004) The timing of snow melt controls the annual CO2 balance in a subarctic fen. *Geophysical Research Letters*, **31**, L16119.

Aurela M, Lohila A, Tuovinen J, Hatakka J, Riutta T, Laurila T (2009) Carbon dioxide exchange on a northern boreal fen. *Boreal Environment Research*, **6095**, 699–710.

Baldocchi D (2008) Breathing of the terrestrial biosphere: lessons learned from a global network of carbon dioxide flux measurement systems. *Australian Journal of Botany*, **56**, 1.

Baldocchi DD, Vogel CA (1997) Seasonal variation of energy and water vapor exchange rates above and below a boreal jack pine forest canopy. *Journal of Geophysical Research*, **102**, 28,939–28951

Baldocchi D, Kelliher FM, Black TA, Jarvis P (2000) Climate and vegetation controls on boreal zone energy exchange. *Global Change Biology*, **6**, 69–83.

Baldocchi D, Falge E, Gu L *et al.* (2001) FLUXNET: a new tool to study the temporal and spatial variability of ecosystem-scale carbon dioxide, water vapor, and energy flux densities. *Bulletin of the American Meteorological Society*, **82**, 2415–2434.

Baldocchi DD, Black TA, Curtis PS *et al.* (2005) Predicting the onset of net carbon uptake by deciduous forests with soil temperature and climate data: a synthesis of FLUXNET data. *International Journal of Biometeorology*, **49**, 377–387.

Barr G, Betts AK, Black TA, Mccaughey JH, Smith CD (2001) Intercomparison of BOREAS northern and southern study area. *Journal of Geophysical Research*, **106**, 543–550.

Barr AG, Black AT, Hogg EH *et al.* (2007) Climatic controls on the carbon and water balances of a boreal aspen forest, 1994-2003. *Global Change Biology*, **13**, 561–576.

Barr AG, van der Kamp G, Black TA, McCaughey JH, Nesic Z (2012) Energy balance closure at the BERMS flux towers in relation to the water balance of the White Gull Creek watershed 1999–2009. *Agricultural and Forest Meteorology*, **153**, 3–13.

Belelli-Marchesini L (2007b) Analysis of the carbon cycle of steppe and old field ecosystems of central Asia, Ph.D. thesis, 209 pp, University of Tuscia, Viterbo, Italy Available at: http://dspace.unitus.it/handle/2067/540 (accessed 15 May 2013).

Belelli-Marchesini L, Papale D, Reichstein M *et al.* (2007a) Carbon balance assessment of a natural steppe of southern Siberia by multiple constraint approach. *Biogeosciences*, **4**, 581–595.

Bergeron O, Margolis HA, Coursolle C, Giasson MA (2008) How does forest harvest influence carbon dioxide fluxes of black spruce ecosystems in eastern North America? *Agricultural and Forest Meteorology*, **148**, 537–548.

Bernier PY, Bartlett P, Black TA, Barr A, Kljun N, McCaughey JH (2006) Drought constraints on transpiration and canopy conductance in mature aspen and jack pine stands. *Agricultural and Forest Meteorology*, **140**, 64–78.

Berninger F, Mäkela A, Hari P (1996) Optimal control of gas exchange during drought: empirical evidence. *Annals of Botany*, **77**, 469–476.

Black TA, den Hartog G, Neumann HH *et al.* (1996) Annual cycles of water vapor and carbon dioxide fluxes in and above a boreal aspen forest. *Global Change Biology*, **2**, 219–229.

Blanken PD, Black TA (2004) The canopy conductance of a boreal aspen forest, Prince Albert National Park, Canada. *Hydrological Processes*, **18**, 1561–1578.

Blanken PD, Black TA, Neumann HH, den Hartog G, Yang PC, Nesic Z, Lee X (2001) The seasonal water and energy exchange above and within a boreal aspen forest. *Journal of Hydrology*, **245**, 118–136.

Blanken PD, Black TA, Yang PC *et al.* (1997) Energy balance and canopy conductance of a boreal aspen forest: partitioning overstory and understory components. *Journal of Geophysical Research*, **102**, 28915–28927.

Boike J, Wille C, Abnizova A (2008) Climatology and summer energy and water balance of polygonal tundra in the Lena River Delta. *Siberia. Journal of Geophysical Research*, **113**, G03025.

Boike J, Kattenstroth B, Abramova K *et al.* (2013) Baseline characteristics of climate, permafrost and land cover from a new permafrost observatory in the Lena River Delta, Siberia (1998–2011). *Biogeosciences*, **10**, 2105–2128.

Bonan GB (2008a) Forests and climate change: forcings, feedbacks, and the climate benefits of forests. *Science*, (New York, N.Y.), **320**, 1444–1449.

Bonan GB (2008b) *Ecological climatology - Concepts and applications*. 2nd edn. Cambride University Press, New York.

Brown SM, Petrone RM, Mendoza C, Devito KJ (2010) Surface vegetation controls on evapotranspiration from a sub-humid Western Boreal Plain wetland. *Hydrological Processes*, **24**, 1072–1085.

Brümmer C, Black TA, Jassal RS *et al.* (2012) How climate and vegetation type influence evapotranspiration and water use efficiency in Canadian forest, peat land and grassland ecosystems. *Agricultural and Forest Meteorology*, **153**, 14–30.

Chapin FS, Mcguire AD, Randerson J *et al.* (2000) Arctic and boreal ecosystems of western North America as components of the climate system. *Global Change Biology*, **6**, 211–223.

Cleugh HA, Leuning R, Mu Q, Running SW (2007) Regional evaporation estimates from flux tower and MODIS satellite data. *Remote Sensing of Environment*, **106**, 285–304.

Corradi C, Kolle O, Walter K, Zimov SA, Schulze E-D (2005) Carbon dioxide and methane exchange of a north-east Siberian tussock tundra. *Global Change Biology*, **11**, 1910–1925.

Coursolle C, Margolis HA, Barr AG *et al.* (2006) Late-summer carbon fluxes from Canadian forests and peatlands along an east – west continental transect. *Canadian Journal of Forest Research*, **800**, 783–800.

Dore S, Montes-Helu M, Hart SC *et al.* (2012) Recovery of ponderosa pine ecosystem carbon and water fluxes from thinning and stand-replacing fire. *Global Change Biology*, **18**, 3171–3185.

Dunn AL, Barford CC, Wofsy SC, Goulden ML, Daube BC (2007) A long-term record of carbon exchange in a boreal black spruce forest: means, responses to interannual variability, and decadal trends. *Global Change Biology*, **13**, 577–590.

Duursma RA, Kolari P, Perämäki M *et al.* (2008) Predicting the decline in daily maximum transpiration rate of two pine stands during drought based on constant minimum leaf water potential and plant hydraulic conductance. *Tree Physiology*, **28**, 265–276.

Epstein HE, Calef MP, Walker MD, Chapin ST III, Starfield AM (2004) Detecting changes in arctic tundra plant communities in response to warming over decadal time scales. *Global Change Biology*, **10**, 1325–1334.

Escobedo JF, Gomes EN, Oliveira AP, Soares J (2011) Ratios of UV, PAR and NIR components to global solar radiation measured at Botucatu site in Brazil. *Renewable Energy*, **36**, 169–178.

Eugster W, Rouse WR, Pielke RA *et al.* (2000) Land-atmosphere energy exchange in Arctic tundra and boreal forest : available data and feedbacks to climate. *Global Change Biology*, **6**, 84–115.

Euskirchen ES, Bret-Harte MS, Cott GJ, Edgar C, Shaver GR (2012) Seasonal patterns of carbon dioxide and water fluxes in three representative tundra ecosystems in northern Alaska. *Ecosphere*, **3**, Article 4 1–19.

Falge E, Baldocchi D, Olson R *et al.* (2001) Gap filling strategies for long term energy flux data sets. *Agricultural and Forest Meteorology*, **107**, 71–77.

Flanagan LB, Syed KH (2011) Stimulation of both photosynthesis and respiration in response to warmer and drier conditions in a boreal peatland ecosystem. *Global Change Biology*, **17**, 2271–2287.

Foken T (2008) The energy balance closure problem: an overview. *Ecological applications*, **18**, 1351–1367.

Garratt JR (1978) Transfer characteristics for a heterogeneous surface of large aerodynamic roughness. *Quarterly Journal of the Royal Meteorological Society*, **104**, 491–502.

Gea-Izquierdo G, Mäkelä A, Margolis H *et al.* (2010) Modeling acclimation of photosynthesis to temperature in evergreen conifer forests. *The New phytologist*, **188**, 175–186.

Gioli B, Miglietta F, De Martino B *et al.* (2004) Comparison between tower and aircraft-based eddy covariance fluxes in five European regions. *Agricultural and Forest Meteorology*, **127**, 1–16.

Göckede M, Foken T, Aubinet M *et al.* (2008) Quality control of CarboEurope flux data – Part 1: coupling footprint analyses with flux data quality assessment to evaluate sites in forest ecosystems. *Biogeosciences*, **5**, 433–450.

Goulden ML, McMillan AMS, Winston GC, Rocha AV, Manies KL, Harden JW, Bond-Lamberty BP (2011) Patterns of NPP, GPP, respiration, and NEP during boreal forest succession. *Global Change Biology*, **17**, 855–871.

Grace J (1990) Cuticular water loss unlikely to explain tree-line in Scotland. *Oecologia*, **84**, 64–68.

Granier A, Reichstein M, Bréda N *et al*. (2007) Evidence for soil water control on carbon and water dynamics in European forests during the extremely dry year: 2003. *Agricultural and Forest Meteorology*, **143**, 123–145.

Grelle A, Lindroth A, Mölder M (1999) Seasonal variation of boreal forest surface conductance and evaporation. *Agricultural and Forest Meteorology*, **99**, 563–578.

Griffis TJ, Black TA, Morgenstern K *et al*. (2003) Ecophysiological controls on the carbon balances of three southern boreal forests. *Agricultural and Forest Meteorology*, **117**, 53–71.

Hamada S, Ohta T, Hiyama T, Kuwada T, Takahashi A, Maximov TC (2004) Hydrometeorological behaviour of pine and larch forests in eastern Siberia. *Hydrological Processes*, **18**, 23–39.

Hollinger DY, Goltz SM, Davidson EA, Lee JT, Tu K, Valentine HT (1999) Seasonal patterns and environmental control of carbon dioxide and water vapour exchange in an ecotonal boreal forest. *Global Change Biology*, **5**, 891–902.

Hollinger DY, Aber J, Dail B *et al*. (2004) Spatial and temporal variability in forest-atmosphere CO2 exchange. *Global Change Biology*, **10**, 1689–1706.

Hu J, Moore DJP, Riveros-Iregui DA, Burns SP, Monson RK (2010) Modeling whole-tree carbon assimilation rate using observed transpiration rates and needle sugar carbon isotope ratios. *The New phytologist*, **185**, 1000–1015.

van Huissteden J, Maximov TC, Dolman A (2005) High methane flux from an arctic floodplain (Indigirka lowlands, eastern Siberia). *Journal of Geophysical Research*, **110**, G02002.

Jarvis PG (1976) The interpretation of the variations in leaf water potential and stomatal conductance found in canopies in the field. *Philosophical Transactions of the Royal Society of London B, Biological Sciences*, **273**, 593–610.

Jarvis PG, Massheder JM, Hale SE, Moncrieff JB, Rayment M, Scott SL (1997) Seasonal variation in carbon dioxide, water vapor, and energy exchanges of a boreal black spruce forest. *Journal of Geophysical Research*, **102**, 28953–28966.

Jasechko S, Sharp ZD, Gibson JJ, Birks SJ, Yi Y, Fawcett PJ (2013) Terrestrial water fluxes dominated by transpiration. *Nature*, **496**, 347–350.

Jassal RS, Black TA, Spittlehouse DL, Brümmer C, Nesic Z (2009) Evapotranspiration and water use efficiency in different-aged Pacific Northwest Douglas-fir stands. *Agricultural and Forest Meteorology*, **149**, 1168–1178.

Jung M, Reichstein M, Bondeau A (2009) Towards global empirical upscaling of FLUXNET eddy covariance observations: validation of a model tree ensemble approach using a biosphere model. *Biogeosciences*, **6**, 2001–2013.

Jung M, Reichstein M, Ciais P *et al*. (2010) Recent decline in the global land evapotranspiration trend due to limited moisture supply. *Nature*, **467**, 951–954.

Jung M, Reichstein M, Margolis HA *et al*. (2011) Global patterns of land-atmosphere fluxes of carbon dioxide, latent heat, and sensible heat derived from eddy covariance, satellite, and meteorological observations. *Journal of Geophysical Research*, **116**, G00J07.

Katul GG, Oren R, Manzoni S, Higgins C, Parlange MB (2012) Evapotranspiration : a process driving mass transport and energy exchange in the soil-plant-atmosphere-climate system. *Reviews of Geophysics*, **50**, RG3002.

Kelliher FM, Leuning R, Raupach MR, Schulze E (1995) Maximum conductances for evaporation vegetation types from global. *Agricultural and Forest Meteorology*, **1923**, 1–16.

Kelliher FM, Lloyd J, Arneth A *et al*. (1998) Evaporation from a central Siberian pine forest. *Journal of Hydrology*, **205**, 279–296.

Kettridge N, Thompson DK, Bombonato L, Turetsky MR, Benscoter BW, Waddington JM (2013) The ecohydrology of forested peatlands: simulating the effects of tree shading on moss evaporation and species composition. *Journal of Geophysical Research: Biogeosciences*, **118**, 422–435.

Kljun AN, Black TA, Griffis TJ *et al*. (2006) Response productivity stands of net of three to ecosystem boreal forest. *Ecosystems*, **9**, 1128–1144.

Kolari P, Lappalainen HK, Hänninen H, Hari P (2007) Relationship between temperature and the seasonal course of photosynthesis in Scots pine at northern timberline and in southern boreal zone. *Tellus B*, **59**, 542–552.

Krishnan P, Black TA, Jassal RS, Chen B, Nesic Z (2009) Interannual variability of the carbon balance of three different-aged Douglas-fir stands in the Pacific Northwest. *Journal of Geophysical Research*, **114**, G04011.

Kurbatova J, Li C, Varlagin A, Xiao X, Vygodskaya N (2008) Modeling carbon dynamics in two adjacent spruce forests with different soil conditions in Russia. *Biogeosciences*, **5**, 969–980.

Kustas WP, Choudhury BJ, Moran MS, Reginato RJ, Jackson RD, Gay LW, Weaver HL (1989) Determination of sensible heat flux over sparse canopy using thermal infrared data. *Agricultural and Forest Meteorology*, **44**, 197–216.

Kustas WP, Goodrich DC, Moran MS *et al*. (1991) An Interdisciplinary Field Study of the Energy and Water Fluxes in the Atmosphere-Biosphere System over Semiarid Rangelands: Description and Some Preliminary Results. *Bulletin of the American Meteorological Society*, **72**, 1683–1705.

Lagergren F, Lindroth A (2002) Transpiration response to soil moisture in pine and spruce trees in Sweden. *Agricultural and Forest Meteorology*, **112**, 67–85.

Lagergren F, Lankreijer H, Kučera J, Cienciala E, Mölder M, Lindroth A (2008) Thinning effects on pine-spruce forest transpiration in central Sweden. *Forest Ecology and Management*, **255**, 2312–2323.

Langer M, Westermann S, Muster S, Piel K, Boike J (2011) The surface energy balance of a polygonal tundra site in northern Siberia – Part 2: winter. *The Cryosphere*, **5**, 509–524.

Launiainen S (2010) Seasonal and inter-annual variability of energy exchange above a boreal Scots pine forest. *Biogeosciences*, **7**, 3921–3940.

Law BE, Falge E, Gu L *et al*. (2002) Environmental controls over carbon dioxide and water vapor exchange of terrestrial vegetation. *Agricultural and Forest Meteorology*, **113**, 97–120.

Lecina S, Martínez-Cob A, Pérez PJ, Villalobos FJ, Baselga JJ (2003) Fixed versus variable bulk canopy resistance for reference evapotranspiration estimation using the Penman–Monteith equation under semiarid conditions. *Agricultural Water Management*, **60**, 181–198.

Leuning R (1995) A critical appraisal of a coupled stomatal–photosynthesis model for C3 plants. *Plant, Cell and Environment*, **18**, 339–357.

Leuning R, van Gorsel E, Massman WJ, Isaac PR (2012) Reflections on the surface energy imbalance problem. *Agricultural and Forest Meteorology*, **156**, 65–74.

Lindroth A, Grelle A, More A (1998) Long-term measurements of boreal forest carbon balance. *Global Change Biology*, **4**, 443–450.

Lindroth A, Lagergren F, Aurela M *et al*. (2008) Leaf area index is the principal scaling parameter for both gross photosynthesis and ecosystem respiration of Northern deciduous and coniferous forests. *Tellus B*, **60**, 129–142.

Liu H, Randerson JT, Lindfors J, Chapin FS III (2005) Changes in the surface energy budget after fire in boreal ecosystems of interior Alaska: an annual perspective. *Journal of Geophysical Research*, **110**, D13101.

Lohila A, Aurela M, Hatakka J, Pihlatie M, Minkkinen K, Penttilä T, Laurila T (2010) Responses of N2O fluxes to temperature, water table and N deposition in a northern boreal fen. *European Journal of Soil Science*, **61**, 651–661.

Lund M, Lindroth A, Christensen TR, Ström L (2007) Annual CO 2 balance of a temperate bog. *Tellus B*, **59**, 804–811.

Lund M, Lafleur PM, Roulet NT *et al*. (2009) Variability in exchange of CO2 across 12 northern peatland and tundra sites. *Global Change Biology*, **16**, 2436–2488.

Mäkelä A, Hari P, Berninger F, Hänninen H, Nikinmaa E (2004) Acclimation of photosynthetic capacity in Scots pine to the annual cycle of temperature. *Tree Physiology*, **24**, 369–376.

Mäkelä A, Kolari P, Karimäki J, Nikinmaa E, Perämäki M, Hari P (2006) Modelling five years of weather-driven variation of GPP in a boreal forest. *Agricultural and Forest Meteorology*, **139**, 382–398.

Mäkelä A, Pulkkinen M, Kolari P *et al*. (2008) Developing an empirical model of stand GPP with the LUE approach: analysis of eddy covariance data at five contrasting conifer sites in Europe. *Global Change Biology*, **14**, 92–108.

Margolis HA, Ryan MG (1997) A physiological basis for biosphere-atmosphere interactions in the boreal forest: an overview. *Tree physiology*, **17**, 491–499.

McCaughey JH, Pejam MR, Arain MA, Cameron DA (2006) Carbon dioxide and energy fluxes from a boreal mixedwood forest ecosystem in Ontario, Canada. *Agricultural and Forest Meteorology*, **140**, 79–96.

Merbold L, Kutsch WL, Corradi C *et al*. (2009) Artificial drainage and associated (CO2/CH4) in a tundra ecosystem. *Global Change Biology*, **15**, 2599–2614.

Mkhabela MS, Amiro BD, Barr AG *et al*. (2009) Comparison of carbon dynamics and water use efficiency following fire and harvesting in Canadian boreal forests. *Agricultural and Forest Meteorology*, **149**, 783–794.

Moffat AM, Papale D, Reichstein M *et al*. (2007) Comprehensive comparison of gap-filling techniques for eddy covariance net carbon fluxes. *Agricultural and Forest Meteorology*, **147**, 209–232.

Mu Q, Zhao M, Running SW (2011) Improvements to a MODIS global terrestrial evapotranspiration algorithm. *Remote Sensing of Environment*, **115**, 1781–1800.

New M, Lister D, Hulme M, Makin I (2002) A high-resolution data set of surface climate over global land areas. *Climate research*, **21**, 1–25.

Nordbo A, Launiainen S, Mammarella I, Leppäranta M, Huotari J, Ojala A, Vesala T (2011) Long-term energy flux measurements and energy balance over a small boreal lake using eddy covariance technique. *Journal of Geophysical Research*, **116**, 1–17.

Ohta T, Maximov TC, Dolman AJ *et al*. (2008) Interannual variation of water balance and summer evapotranspiration in an eastern Siberian larchforest over a 7-year period (1998–2006). *Agricultural and Forest Meteorology*, **148**, 1941–1953.

Papaioannou G, Papanikolaou N, Retalis D (1993) Relationships of photosynthetically active radiation and shortwave irradiance. *Theoretical and Applied Climatology*, **48**, 23–27.

Peichl M, Brodeur JJ, Khomik M, Arain MA (2010) Biometric and eddy-covariance based estimates of carbon fluxes in an age-sequence of temperate pine forests. *Agricultural and Forest Meteorology*, **150**, 952–965.

Peichl M, Sagerfors J, Lindroth A *et al.* (2013) Energy exchange and water budget partitioning in a boreal minerogenic mire. *Journal of Geophysical Research: Biogeosciences*, **118**, 1–13.

Penman HL (1948) Natural evaporation from open water, bare soil and grass. *Proceedings of the Royal Society London Academy*, **193**, 120–146.

Pilegaard K, Hummelshøj P, Jensen N, Chen Z (2001) Two years of continuous CO_2 eddy-flux measurements over a Danish beech forest. *Agricultural and Forest Meteorology*, **107**, 29–41.

Pilegaard K, Mikkelsen TN, Beier C, Jensen NO, Abmus P, Ro-Poulsen H (2003) Field measurements of atmosphere – biosphere interactions in a Danish beech forest. *Boreal Environment Research*, **8**, 315–333.

R Core Team (2013) R: A language and environment for statistical computing. R Foundation for Statistical Computing, Vienna, Austria. ISBN 3-900051-07-0, Available at: http://www.R-project.org/ (accessed 3 January 2013)

Raulier F, Bernier PY (2000) Predicting the date of leaf emergence for sugar maple across its native range. *Canadian Journal of Forest Research*, **30**, 1429–1435.

Reichstein M, Falge E, Baldocchi D *et al.* (2005) On the separation of net ecosystem exchange into assimilation and ecosystem respiration: review and improved algorithm. *Global Change Biology*, **11**, 1424–1439.

Richardson AD, Black TA, Ciais P *et al*. (2010) Influence of spring and autumn phenological transitions on forest ecosystem productivity. *Philosophical Transactions of the Royal Society of London. Series B, Biological Sciences*, **365**, 3227–3246.

Richardson AD, Anderson RS, Arain MA *et al.* (2012) Terrestrial biosphere models need better representation of vegetation phenology: results from the North American Carbon Program Site Synthesis. *Global Change Biology*, **18**, 566–584.

Richardson AD, Keenan TF, Migliavacca M, Ryu Y, Sonnentag O, Toomey M (2013) Climate change, phenology, and phenological control of vegetation feedbacks to the climate system. *Agricultural and Forest Meteorology*, **169**, 156–173.

Rocha AV, Shaver GR (2011) Burn severity influences postfire CO2 exchange in arctic tundra. *Ecological applications: a publication of the Ecological Society of America*, **21**, 477–489.

Rouse WR (1984) Microclimate of arctic tree line 2. soil microclimate of tundra and forest. *Water Resources Research*, **20**, 67–73.

Rouse WR (2000) The energy and water balance of high-latitude wetlands: controls and extrapolation. *Global Change Biology*, **6**, 59–68.

Running SW (1980) Relating plant capacitance to the water relations of Pinus contorta. *Forest Ecology and Management*, **24**, 237–252.

Sellers PJ, Dickinson RE, Randall DA *et al.* (1997) Modeling the exchanges of energy, water, and carbon between continents and the atmosphere. *Science*, **275**, 502–509.

Sellers APJ, Bounoua L, Collatz GJ *et al.* (2009) Comparison of radiative and physiological effects of doubled atmospheric CO_2 on climate. *Science*, **271**, 1402–1406.

Sevanto S, Suni T, Pumpanen J *et al.* (2006) Wintertime photosynthesis and water uptake in a boreal forest. *Tree Physiology*, **26**, 749–757.

Shuttleworth W, Wallace J (1985) Evaporation from sparse crops-an energy combination theory. *Quarterly Journal of the Royal Meteorological Society*, **111**, 839–855.

Stewart JB (1988) Modelling surface conductance of pine forest. *Agricultural and Forest Meteorology*, **43**, 19–35.

Stoy PC, Richardson AD, Baldocchi DD *et al.* (2009) Biosphere-atmosphere exchange of CO_2 in relation to climate: a cross-biome analysis across multiple time scales. *Biogeosciences*, **6**, 2297–2312.

Stoy PC, Mauder M, Foken T *et al*. (2013) A data-driven analysis of energy balance closure across FLUXNET research sites: the role of landscape scale heterogeneity. *Agricultural and Forest Meteorology*, **171–172**, 137–152.

Suni T, Berninger F, Vesala T *et al*. (2003) Air temperature triggers the recovery of evergreen boreal forest photosynthesis in spring. *Global Change Biology*, **9**, 1410–1426.

Tanaka H, Hiyama T, Kobayashi N *et al*. (2008) Energy balance and its closure over a young larch forest in eastern Siberia. *Agricultural and Forest Meteorology*, **148**, 1954–1967.

Tchebakova NM, Kolle O, Zolotoukhine D *et al.* (2002) Inter-annual and seasonal variations of energy and water vapour fluxes above a Pinus sylvestris forest in the Siberian middle taiga. *Tellus B*, **54**, 537–551.

Thum T, Aalto T, Laurila T, Aurela M, Kolari P, Hari P (2007) Parametrization of two photosynthesis models at the canopy scale in a northern boreal Scots pine forest. *Tellus B*, **59**, 874–890.

Troufleau D, Lhomme JP, Monteny B, Vidal A, Moran MS (1995) Using thermal infrared temperature over sparse semi-arid vegetation for sensible heat flux estimation. In: *Geoscience and Remote Sensing Symposium*, 1995. IGARSS 95. "Quantitative Remote Sensing for Science and Applications", International, Firenze, Italy (ed. Stein TI), pp. 2227–2229. Institute of Electrical and Electronics Engineers, New York. Available at: http://ieeexplore.ieee.org/stamp/stamp.jsp?tp=&arnumber=524155&isnumber=11411 (accessed 1 June 2013).

Urbanski S, Barford C, Wofsy S *et al.* (2007) Factors controlling CO_2 exchange on timescales from hourly to decadal at Harvard Forest. *Journal of Geophysical Research*, **112**, G02020.

Valiantzas JD (2006) Simplified versions for the Penman evaporation equation using routine weather data. *Journal of Hydrology*, **331**, 690–702.

Verma SB (1989) Aerodynamic resistances for transfer of mass, heat and momentum. In: *Estimation of Aerial Evapotranspiration* (Proceedings of a workshop held at Vancouver, B.C. Canada, August 1987), IAHS Publication no. 177, 1989 (ed. Black TA), pp. 13–20. IAHS Press, Wallingford.

Vesala T, Suni T, Rannik U *et al.* (2005) Effect of thinning on surface fluxes in a boreal forest. *Global Biogeochemical Cycles*, **19**, 1–12.

Walker DA, Jia GJ, Epstein HE *et al.* (2003) Vegetation-soil-thaw-depth relationships along a low-arctic bioclimate gradient, Alaska: synthesis of information from the ATLAS studies. *Permafrost and Periglacial Processes*, **14**, 103–123.

Wang C, Bond-Lamberty B, Gover ST (2003) Carbon distribution of a well- and poorly-drained black spruce fire chronosequence. *Global Change Biology*, **9**, 1066–1079.

Wang K, Dickinson RE (2012) A review of global terrestrial evapotranspiration: observation, modeling, climatology, and climatic variability. *Reviews of Geophysics*, **50**, 1–54.

Weiss A, Norman JM (1985) Partitioning solar radiation into direct and diffuse, visible and near-infrared components. *Agricultural and Forest Meteorology*, **34**, 205–213.

Wieser G (2000) Seasonal variation of leaf conductance in a subalpine *Pinus cembra* during the winter months. *Phyton - Annales Rei Botanicae*, **40**, 185–190.

Wilson K, Goldstein A, Falge E *et al.* (2002) Energy balance closure at FLUXNET sites. *Agricultural and Forest Meteorology*, **113**, 223–243.

Wong SC, Cowan IR, Farquhar GD (1979) Stomatal conductance correlates with photosynthetic capacity. *Nature*, **282**, 424–426.

Wu A, Black TA, Verseghy DL, Blanken PD, Novak MD, Chen W, Yang PC (2000) A comparison of parameterizations of canopy conductance of aspen and Douglas-fir forests for CLASS. *Atmosphere-Ocean*, **38**, 81–112.

Wu J, Kutzbach L, Jager D, Wille C, Wilmking M (2010) Evapotranspiration dynamics in a boreal peatland and its impact on the water and energy balance. *Journal of Geophysical Research*, **115**, G04038.

Yuan F, Arain MA, Barr AG *et al.* (2008) Modeling analysis of primary controls on net ecosystem productivity of seven boreal and temperate coniferous forests across a continental transect. *Global Change Biology*, **14**, 1765–1784.

Zha T, Barr AG, van der Kamp G, Black TA, McCaughey JH, Flanagan LB (2010) Interannual variation of evapotranspiration from forest and grassland ecosystems in western canada in relation to drought. *Agricultural and Forest Meteorology*, **150**, 1476–1484.

Supporting Information

Additional Supporting Information may be found in the online version of this article:

Appendix S1. The calibrated best-fit model parameters for the sites used in the study and proportion of explained variance (PR^2), bias, root-mean-square-error (RMSE) and measured mean (MM) of the model in half hour, daily and monthly time scale. Calibrated model and statistical parameters for different vegetation types are presented in the end of the table (C, cutter/open/burned forest; D, Douglas-Fir; G, grass; L, larch, BD, broadleaf deciduous forest; P, pine; S, spruce; T, tundra; W, wetland/mire/bog). The amount of 30 min data points for the site or ecosystem is reported in the column Rows.